the higher order functions. To find these, we choose a set of $2n$ coordinates at random and let A be any operator of the form

$$A=\lambda_1 E^{(+)}(x_1)\cdots E^{(+)}(x_n) +\lambda_2 E^{(+)}(x_{n+1})\cdots E^{(+)}(x_{2n}). \quad \text{(A12)}$$

The positive definiteness of the quadratic form which results from substituting this expression in (A1) shows that the inequality (3.14) must hold. When vector indices are attached to the operators $E^{(+)}$, the same proof leads to (5.11).

We have noted in the text that, for the particular case of coherent fields, the inequalities of second degree in the correlation functions reduce to equalities. The reason for the reduction lies in the way the correlation functions factorize. The factorization causes all of the second and higher order determinants involved in the statement of positive definiteness conditions [e.g., (A9)] to vanish.

PHYSICAL REVIEW VOLUME 130, NUMBER 6 15 JUNE 1963

Statistical Mechanical Theory of Condensation*

M. COOPERSMITH† AND R. BROUT‡
Laboratory of Atomic and Solid State Physics and Department of Physics, Cornell University, Ithaca, New York
(Received 6 July 1962; revised manuscript received 9 October 1962)

The cluster expansion for the free energy of the Ising model is reinterpreted as a cluster expansion for the pressure of the lattice gas. It is observed that the free energy of the Ising model is a function of $1-R^2$, where R is the long-range order, so that the pressure of the lattice gas is a function of $\rho(1-\rho)$, where ρ is density. The factor $1-\rho$ comes from the prevention of more than one particle occupying a lattice site. This idea has motivated the development of a real hard-core gas with a weak attractive tail. A cluster expansion is developed in terms of the tail alone and the hard core is treated as a metric (i.e., the hard-core part of the potential is treated exactly in all integrals). Pressure-volume isotherms are calculated explicitly in the zeroth order or molecular field approximation using the Lennard-Jones (6–12) potential and good quantitative results are found for the critical parameters as well as a qualitative understanding of the condensation phenomena. The theory of the first-order correction (spherical model) is then outlined and fluctuations of the Ornstein-Zernicke type in the local density are found. The theory of condensation is qualitatively understood in the sense that the Weiss field gives an understanding of ferromagnetism. The theory of the detailed fluctuations in the critical region is equally difficult for both phenomena since the problems are put on the same footing in the present paper.

I. INTRODUCTION

IN a series of papers, Brout and Horwitz[1] have shown how to obtain a linked cluster expansion for the Ising model and, in particular, how to calculate the spherical model value for the free energy as a high-density limit of the cluster expansion. We note the trivial but important fact that the spherical model value of the free energy below the Curie point is a function of $1-R^2$, where R is the long-range order of magnetization. Reinterpreting the free energy of the Ising model as the pressure of a lattice gas in the manner of Lee and Yang,[2] we observe that the lattice gas pressure is a function of $\rho(1-\rho)$, where ρ is the density. Since the factor $1-\rho$ comes about from the fact that no more than one particle is allowed on a lattice site (hard core), we conjecture that it might be profitable to formulate a cluster expansion for a real hard-core gas with a weak attractive tail using the tail alone as the perturbation and calculating all ensemble averages with the hard core as a metric (i.e., the cluster integrals which occur contain the hard sphere part exactly taking into account no overlapping of the cores).

In Sec. II, we review briefly the cluster expansion for the Ising model and the high-density limit (spherical model) as a sum of ring graphs (random phase approximation). In Sec. III, we present this cluster expansion by a method which uses the lattice gas interpretation of the Ising model rather than the conventional spin method. The advantage of this method is that the cluster expansion for a real gas with a hard core can be developed in a parallel manner. In Sec. IV, we show how to formulate this linked cluster expansion for an imperfect hard-core gas. Finally, in Sec. V we calculate the pressure-volume isotherms for the real gas using the zeroth order of molecular field approximation to the

* Supported in part by the Office of Naval Research.
† This paper is abstracted from the dissertation of M. Coopersmith submitted to Cornell University in partial fulfillment for the requirements of the doctoral degree. National Science Postdoctoral Fellow 1961–1962. Present address: Institute for the Study of Metals, University of Chicago, Chicago, Illinois.
‡ John Simon Guggenheim Fellow 1961–1962. Present address: Université Libre de Bruxelles, Brussels, Belgium.
[1] R. Brout, Phys. Rev. **115**, 824 (1959); **118**, 1009 (1960); **122**, 469 (1961); G. Horwitz and H. Callen, *ibid.* **124**, 1757 (1961). Hereafter referred to as I, II, III, and IV, respectively.
[2] T. D. Lee and C. N. Yang, Phys. Rev. **87**, 410 (1952); **87**, 404 (1952).

cluster expansion. By formally summing the set of spherical model ring graphs, we then show how to obtain fluctuations of the Ornstein-Zernicke[3] type.

Because the fundamental idea is simple, but the formal manipulations tedious and sometimes difficult, we have put all formal cluster developments into a series of Appendixes. The physical content of the paper is obtainable without reading these Appendices.

II. REVIEW OF ISING MODEL OF FERROMAGNETISM

In this section we recall briefly some of the results known in the theory of the three-dimensional Ising model. The point of view is that expressed in the papers of reference 1. This set of works is incomplete and we are still very far from a thorough quantitative understanding of the three-dimensional phase transition phenomena. However, we have obtained certain qualitative understanding from the above-mentioned development. It is to be hoped that this point of view will eventually be juxtaposed with the numerical work of Domb and Sykes[4] based on a term by term moment expansion of the free energy. The advantage of the latter method is a precise quantitative estimate of critical point behavior. The disadvantage is lack of a "physical picture," balance of energy and entropy, etc. Our present point of view is to achieve a qualitative understanding of condensation paralleling that of ferromagnetism.

We first review the molecular theory approximation of the Ising model. The Hamiltonian in the notation of reference 1 is

$$H=-\tfrac{1}{2}\sum_{i\neq j} v_{ij}\mu_i\mu_j-\sum \mu_i\mathcal{H}. \tag{2.1}$$

The Weiss theory makes the fundamental assumption of statistical independence.

$$\langle\mu_i\mu_j\rangle=\langle\mu_i\rangle\langle\mu_j\rangle. \tag{2.2}$$

Alternatively, each spin feels a mean field

$$\langle\mathcal{H}_{\text{mol}}\rangle=\sum_{j=1}^{N_0} v_{ij}\langle\mu_j\rangle+\mathcal{H}=v(0)R+\mathcal{H}, \tag{2.3}$$

where R is the magnetization and is equal to $\langle\mu_i\rangle$ ensemble average. The energy is then given by

$$E=-\tfrac{1}{2}N_0v(0)R^2-N_0\mathcal{H}R, \tag{2.4}$$

where $v(0)$ is the $q=0$ component of the Fourier transform of the exchange integral. The Weiss theory becomes exact in the limit of an exchange integral of infinite range. One calculates the free energy as $E-TS$ where for S one uses the entropy of spins distributed at random but at fixed R. Using the stationarity of F with respect to R, we arrive at the familiar molecular field theory equation for the magnetization as a function of an applied magnetic field H.

$$R=\tanh[\beta(v(0)R+\mathcal{H})]. \tag{2.5}$$

From Eq. (2.6) we find that the Curie temperature is given by

$$kT_c=v(0). \tag{2.6}$$

Equation (2.5) contains all the qualitative features of ferromagnetism except a description of short-range order, i.e., microscopic deviations in the long-range order or magnetization. This is, of course, a direct result of using a molecular field which is constant at all spin sites. If the exchange potential is now considered to be cut off at a finite distance (nearest-neighbor distance in a crystal lattice is the usual procedure), then it can easily be seen that the molecular field result is a high-z approximation, where z is the number of spins in the range of the potential. This result, as well as the expansion of the free energy in powers of $1/z$ (cluster expansion), is described in II.

In III, it was shown that the summation of ring diagrams with noncrossing internal dotted lines is equivalent to the spherical model of Berlin and Kac.[5] The Curie point is reduced from the Weiss model by $O(1/z)$ according to

$$kT_c=w(0), \tag{2.8}$$

where $w(\mathbf{q})=v(\mathbf{q})-\delta$ and the saddle parameter, δ, is given by the spherical condition

$$\textstyle\sum_{\mathbf{q}}[1-\beta(1-R^2)w(\mathbf{q})]^{-1}=N. \tag{2.9}$$

$v(\mathbf{q})$ is the crystal Fourier transform of v_{ij}. A recently discovered inconsistency[6] in the spherical model indicates that the fluctuation, $\langle\mu_0^2\rangle-\langle\mu_0\rangle^2$, is not equal to the susceptibility (defined as dR/dH) for zero applied magnetic field below the Curie point as it should be from statistical mechanical considerations, although the singularities occur at the same (Curie) temperature defined in Eq. (2.8). This inconsistency occurs within $O(1/z^2)$ of the Curie point. Detailed examination by Englert and Horwitz[6] has shown that one can reduce the domain of inconsistency by bond renormalization. However, the current status of consistency is by no means clear. In this paper we shall ignore this problem since the main point is to bring the knowledge of condensation as based on cluster developments to a qualitative understanding analogous to the Ising model problem.

III. THREE-DIMENSIONAL LATTICE GAS

The Hamiltonian for the interaction in the Ising model may be written as

$$\mathcal{H}=-\tfrac{1}{2}\sum_{i\neq j}^{N_0} v_{ij}\mu_i\mu_j-N_0R\mathcal{H}, \tag{3.1}$$

[3] L. Ornstein and F. Zernicke, Proc. Acad. Sci. Amsterdam **17**, 793 (1914); Physik Z. **19**, 134 (1918).

[4] For a review of this work see C. Domb, in *Advances in Physics*, edited by N. F. Mott (Taylor and Francis, Ltd., London, 1960), Vol. 9, p. 191. For the applications of this work to critical phenomena see M. Fisher, Physica **28**, 172 (1962).

[5] T. Berlin and M. Kac, Phys. Rev. **86**, 821 (1952).

[6] F. Englert and G. Horwitz (private communication); some results will be found in F. Englert, Phys. Rev. **129**, 567 (1963).

where N_0 is the number of lattice sites or volume of the crystal. In order to establish the connection between the Ising model and the lattice gas, we add to the Hamiltonian the constant $\frac{1}{2}N_0v(0)+N_0\mathfrak{IC}$, where $v(0)$ is the $q=0$ component of the Fourier transform of v_{ij}. The Hamiltonian becomes

$$H_{\text{L.G.}}=-\tfrac{1}{2}\sum_{i\neq j}v_{ij}\mu_i\mu_j-\tfrac{1}{2}N_0v(0)-N_0R\mathfrak{IC}+N_0\mathfrak{IC}. \quad (3.2)$$

We now define

$$\begin{aligned}\rho&\equiv(1-R)/2,\\ \epsilon_i&\equiv(1-\mu_i)/2,\end{aligned} \quad (3.3)$$

or equivalently

$$\begin{aligned}R&=(1-2\rho),\\ \mu_i&=(1-2\epsilon_i),\end{aligned} \quad (3.4)$$

so that ϵ_i takes on the values $+1$ and 0. In terms of the new variables ϵ_i and ρ, the Hamiltonian becomes

$$\begin{aligned}H_{\text{L.G.}}&=-\tfrac{1}{2}\sum_{i\neq j}^{N_0}v_{ij}(\mu_i\mu_j-1)+N_0(1-R)\mathfrak{IC}\\ &=-\tfrac{1}{2}\sum_{i\neq j}^{N_0}v_{ij}(-2\epsilon_i-2\epsilon_j+4\epsilon_i\epsilon_j)+2N_0\rho\mathfrak{IC}\\ &=-2\sum_{i\neq j}^{N_0}v_{ij}\epsilon_i\epsilon_j+2N_0\rho\mathfrak{IC}+2N_0\rho v(0)\\ &=-\tfrac{1}{2}\sum_{i\neq j}^{N_0}u_{ij}\epsilon_i\epsilon_j-N_0\rho\mu,\end{aligned} \quad (3.5)$$

where we have put $u_{ij}=4v_{ij}$ and $\mu=-[2\mathfrak{IC}+u(0)/2]$. Interpreting ρ as the density and μ as the chemical potential, we find that the pressure (ln of the grand partition function) of the lattice gas is equivalent to the free energy of the Ising model as follows:

$$\begin{aligned}-\beta F_I-\tfrac{1}{2}N_0\beta v(0)-N_0\beta\mathfrak{IC}&=N_0\ln Z_I-\tfrac{1}{2}N_0\beta v(0)-N_0\beta\mathfrak{IC}\\ &=\ln\{\sum_{R=1}^{+1}\sum_{\{\mu_i\}}\exp[\tfrac{1}{2}\beta\sum_{i\neq j}^{N_0}v_{ij}\mu_i\mu_j+N_0\beta R\mathfrak{IC}]\}\\ &\qquad-\tfrac{1}{2}N_0\beta v(0)-N_0\beta\mathfrak{IC}\\ &=\ln\{\sum_{\rho=0}^{1}\sum_{\{\epsilon_i\}}\exp[\tfrac{1}{2}\beta\sum_{i\neq j}^{N_0}u_{ij}\epsilon_i\epsilon_j+N_0\beta\rho\mu\}\\ &=\ln\{\sum_{N=0}^{N_0}\sum_{\text{configurations}}\exp[\tfrac{1}{2}\beta\sum_{i\neq j}u_{ij}+N\beta\mu]\}\\ &=\ln\Xi_{\text{L.G.}}=[\beta pV]_{\text{L.G.}}=[\beta pv_aN_0]_{\text{L.G.}},\end{aligned} \quad (3.6)$$

where v_a is the volume of a unit cell of the lattice and a configuration of particles refers to an arrangement with the particles considered as indistinguishable, and p is the pressure. Clearly, the sum over configurations of $\exp[\frac{1}{2}\beta\sum u_{ij}]$ is equivalent to a sum over $\{\epsilon_i\}$ of $\exp[\frac{1}{2}\beta\sum u_{ij}\epsilon_i\epsilon_j]$ since the sum in the exponent of the first expression ranges from 1 to N and the sum in the exponent of the second expression ranges from 1 to N_0.

Using Eq. (3.6), a cluster expansion for the Ising model may be derived. The motivation will become clear when we attempt a study of real gas with hard cores. We first rewrite Eq. (3.6):

$$\ln\Xi=\ln\sum_{N=0}^{N_0}(1/N!)\times\sum_{\text{configurations}}{}'\exp[\tfrac{1}{2}\beta\sum_{i\neq j}u_{ij}+N\beta\mu]. \quad (3.7)$$

The factor $1/N!$ appears here in order to make the connection later on with the real gas. The prime on the sum over configurations indicates that we must include all possible permutations of the particles in a given configuration on the lattice. The $1/N!$ changes the summation over configurations from one involving only combinations to one involving both combinations and permutations.

Following the procedure used in the derivation of the cluster expansion for the Ising model (I), we replace the summation over N by its largest term, say $\bar{N}$. This amounts to picking a fixed $\rho=(N/N_0)$ or, equivalently, using a canonical ensemble instead of a grand ensemble. In the future, since N and $\bar{N}$ will never be used together, we shall drop the bar over the N and replace $\bar{N}$ by N in all equations. Equation (3.7) becomes

$$\ln\Xi=\ln W(\rho)+\ln\langle\exp(\tfrac{1}{2}\beta\sum_{i\neq j}^{N}u_{ij})\rangle+N\beta\mu, \quad (3.8)$$

where $W(\rho)=\binom{N_0}{N}$ and the average of a function, O, of the u's is given by

$$\langle O\rangle\equiv\frac{1}{W(\rho)}\sum_{\text{configurations}}O. \quad (3.9)$$

In writing the above expression for $W(\rho)$, we are making the assumption that no two particles can go on the same lattice site (hard core). The function $W(\rho)$ has the same value as the function $W(R)$ used in the Ising model when ρ is given by Eq. (3.3) in terms of R. We now write the logarithm of the average of the exponential as a semi-invariant expansion.[1]

$$\ln\langle\exp(\tfrac{1}{2}\beta\sum_{i\neq j}\mu_{ij})\rangle=\sum_{n=1}^{\infty}(\beta^n/n!)M_n(\tfrac{1}{2}\sum_{i\neq j}^{N}u_{ij}), \quad (3.10)$$

and proceed in the manner of the articles of reference 1. As the cluster expansion so obtained is a re-expression of the results of the reference 1, we relegate the details of proof to Appendix A.

The reason for presenting this new proof of already familiar results is that the development of the real gas is carried out along exactly analogous lines. The reader

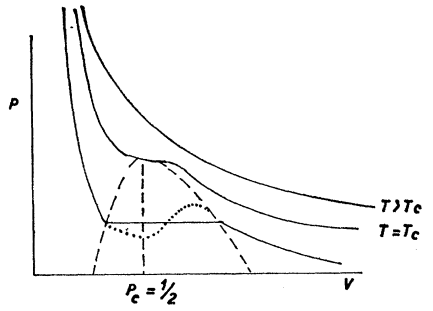

FIG. 1. Pressure-volume isotherms (schematic) in molecular field theory approximation of the Ising model.

interested in the details of the cluster developments of the real gas (Appendix B) as carried out in this paper is first advised to practice on the Ising model as given in Appendix A.

The results of the cluster development of the second term on the right-hand side of Eq. (3.8) is that the coefficient of $\beta^n/n!$ is the sum of all irreducible graphs containing n solid lines as well as internal noncrossing dashed lines with the proviso that if a graph is pinched together where there is a dashed line (i.e., two vertices connected by a dashed line are juxtaposed), then the resulting graph must be reducible. To calculate the value of a graph, one associates to each solid line between vertices i and j a factor $-u_{ij}$ and to each dashed line a factor $-\delta_{ij}$. To a vertex joined by ν solid lines, one associates a factor $M_\nu(\rho)$ which is the νth semi-invariant generated by ρ. One multiplies these factors together and sums on all possible such graphs.

In analogy with the Weiss theory of ferromagnetism, we investigate the theory resulting from taking only the first diagram in the cluster expansion. (In the Horwitz-Callen formulation, this is the summation on Cayley trees.) This is

$$\tfrac{1}{2}\rho^2 \sum_{r_1,r_2=1}^{N_0} u_{r_1r_2}g_{r_1r_2}=\tfrac{1}{2}N_0\rho^2u(0). \tag{3.11}$$

The pressure is then given by

$$\frac{1}{\beta}\ln\Xi=pN_0=(1/\beta)\ln W(\rho) +\tfrac{1}{2}N_0\rho^2u(0)+N_0\rho\mu. \tag{3.12}$$

To determine ρ as a function of μ we use the stationary property of the pressure with respect to ρ in analogy with the molecular field treatment of the Ising model. We get

$$\partial pN_0/\partial\rho=(N_0/\beta)\ln[(1-\rho)\rho] +N_0\rho u(0)+N_0\mu=0, \tag{3.13}$$

or

$$\rho=\tfrac{1}{2}\{\tanh[\tfrac{1}{2}(\beta\rho u(0)+\beta\mu)]+1\}. \tag{3.14}$$

Eliminating μ from Eq. (3.12) by using Eq. (3.13), we obtain for the pressure

$$\begin{aligned} pN_0&=(1/\beta)[-N_0\rho\ln\rho-N_0(1-\rho)\ln(1-\rho)] \\ &\quad+\tfrac{1}{2}N_0\rho^2u(0)+(1/\beta)[N_0\rho\ln\rho \\ &\quad-N_0\rho\ln(1-\rho)]-N_0\rho^2u(0) \\ &=-(N_0/\beta)\ln(1-\rho)+\tfrac{1}{2}\rho^2u(0). \end{aligned} \tag{3.15}$$

In Fig. 1, we show the pressure-volume isotherms schematically for three values of the temperature. Again, as in the Ising model molecular field, we have a loop in the isotherm for $T<T_c$. The straight line is the result of using a grand ensemble instead of a canonical ensemble as we have done by fixing N. The dashed line represents the coexistence curve of liquid and vapor and is a transformation of the magnetization curve from the Ising model. In fact, the isotherms could have been obtained by simply transforming Eq. (1.6) using Eqs. (3.4) and (3.6). We use the above method, however, to establish a connection later on with the real gas. The critical temperature is determined as the largest value of the temperature for which the compressibility, $\partial p/\partial v=0$. Since $\partial p/\partial\rho$ is zero when $\partial p/\partial v$ is zero, we see easily from Eq. (3.15) that

$$kT_c=u(0)/4. \tag{3.16}$$

This is the same as Eq. (2.7) for the molecular field theory of ferromagnetism when it is remembered that $u(0)=4v(0)$.

It should be mentioned at this point that according to Eq. (3.3) defining ρ in terms of R, we have the simple but very important equation

$$\tfrac{1}{4}(1-R^2)=\rho(1-\rho). \tag{3.17}$$

The free energy in the Ising model apart from the magnetic field is an even function of R since the Hamiltonian is invariant under $\mu_i\rightarrow-\mu_i$. Consequently, the free energy can always be written as a function of $1-R^2$ which means that the pressure of the lattice gas is a function of $\rho(1-\rho)$. Furthermore, the cluster expansion is in terms of $\rho(1-\rho)$,[1] which means that if we consider small densities (gas), we have an expansion in terms of ρ or the number of particles since $1-\rho$ is essentially unity. Similarly if we consider densities close to unity (liquid), then we have an expansion in terms of $1-\rho$ or the number of holes. It is easily seen that preventing the particles in the lattice gas from occupying the same lattice sites (hard cores) gives rise to the factor $1-\rho$ which is not present in the original Mayer cluster expansion where the whole interaction potential, hard core included, is used as the perturbation. This leads to an expansion in terms of ρ alone. The importance of the expansion parameter $\rho(1-\rho)$ is stressed since it will motivate our thinking when we come to the real gas.

For completeness, we present the spherical model for the lattice gas. Although it is subject to the same inconsistency as the spherical model for the Ising

model, it nevertheless gives an indication of how to obtain fluctuations in the theory of the real gas. Since the diagrams contributing to the spherical model in the present case are the same as those contributing to the spherical model of ferromagnetism, we shall simply transcribe the equations for ferromagnetism into those for the lattice gas without rederiving them. We shall, however, derive the analogous theory for the real gas. The equation for the free energy of the Ising model in II yields for the pressure of the lattice gas.

$$\beta p N_0 = \ln W(\rho) + \tfrac{1}{2} N_0 \beta \rho^2 u(0) - \tfrac{1}{2} \sum_{\mathbf{q}\neq 0} \ln[1-\beta\rho(1-\rho)z(\mathbf{q})] + \tfrac{1}{2} N_0 \rho(1-\rho)\beta\epsilon + N_0\rho\beta\mu, \quad (3.18)$$

where $z(\mathbf{q})=u(\mathbf{q})-\epsilon$ and ϵ is the saddle parameter. The equation determining ϵ is given by transforming Eq. (2.9).

$$\sum_{\mathbf{q}\neq 0} [1-\beta\rho(1-\rho)z(\mathbf{q})] = N_0. \quad (3.19)$$

The interpretation of Eq. (3.19) is the following. We write the interaction energy of the lattice gas as

$$\tfrac{1}{2} \sum_{i\neq j}^{N_0} u_{ij}\epsilon_i\epsilon_j = \tfrac{1}{2} \sum_{\mathbf{q}} u(\mathbf{q}) |\epsilon(\mathbf{q})|^2, \quad (3.20)$$

where the Fourier transform of ϵ_i is defined in the same way as for μ_i in the Ising model. Now,

$$\sum_{\mathbf{q}\neq 0} |\epsilon_{\mathbf{q}}|^2 = \sum_{\mathbf{q}} |\epsilon_{\mathbf{q}}|^2 - \epsilon_0^2 = \sum_{i=1}^{N_0} \epsilon_i^2 - \frac{1}{N_0} \sum_{i,j=1}^{N_0} \epsilon_i\epsilon_j = N_0\rho(1-\rho). \quad (3.21)$$

But $\langle |\epsilon_{\mathbf{q}}|^2 \rangle$ is given by

$$\langle |\epsilon_{\mathbf{q}}|^2 \rangle = 2\partial \ln \Xi / \partial \beta u(\mathbf{q}) = \rho(1-\rho)/[1-\beta\rho(1-\rho)z(\mathbf{q})], \quad (3.22)$$

so that Eq. (3.19) for the saddle parameter just expresses the spherical condition, Eq. (3.21). The phase transition is the place where $|\epsilon_0|^2 \to \infty$, i.e., the compressibility blows up. This occurs at unique values of ρ and T, namely,

$$\rho_c = \tfrac{1}{2}, \quad kT_c = z(0). \quad (3.23)$$

The critical density ρ_c in this case is determined by symmetry alone.

If it were not for the rapid variation of $\epsilon(T,\rho)$ with ρ within $(1/z)$ of T, the theory based on Eq. (3.22) would describe condensation very neatly. Actually the critical region is very badly handled because of the inconsistency mentioned in Sec. I.

Let us, however, assume that this difficulty did not arise; for example, suppose one could suppress the variation of ϵ with ρ in the critical region for some reason or another [actually it has been shown that this suppression occurs to $O(1/z)$ and is probably general[6]], then it is clear that the presence of the factor $\rho(1-\rho)$ in (3.22) for $\beta>\beta_c$ leads to convergent results in the liquid phase ($\rho>\frac{1}{2}$). In this way, an equation of state based on (3.18) presents a convergent expansion in terms of the parameter $\rho(1-\rho)$ which describes at once both liquid and vapor, in the same way that the Ising model factor $(1-R^2)$ gives a convergence factor in the presence of both $\pm\mathfrak{M}$ (in the limit as $|\mathfrak{M}| \to 0$ for $\beta>\beta_c$).

IV. THREE-DIMENSIONAL HARD-CORE GAS WITH WEAK ATTRACTIVE TAIL

The motivation for dealing with a hard-core gas is the success of the factor $1-\rho$ in determining an equation of state which is valid for the liquid and gas regions below the critical temperature in the lattice gas. The idea will be to use the hard core as the unperturbed part of the Hamiltonian and the weak attractive tail as the perturbation.[7] As with the lattice gas, the cluster expansion will be made on the attractive interaction averaged over the unperturbed hard-core interaction. The following notation will be used throughout the rest of this paper:

V=volume of system, N=number of particles, N_0 =maximum number of particles in the volume, V, a=diameter of hard core, $v_a=a^3/\sqrt{2}$=volume of each particle in close-packed arrangement, ρ=density, $\rho v_a = N/N_0$, $g^{(n)}(r)=n$-particle hard-core correlation function, $\tilde{f}(r)=1-g^{(2)}(r)$, $v_{\text{H.C.}}(r)$=hard-core potential.

The logarithm of the grand partition function is

$$\ln\Xi = \ln \sum_{N=0}^{N_0} [\exp(\beta\mu N)/N!] \times \int\cdots\int \prod d^3r_i \exp[-\tfrac{1}{2}\beta \sum u_{ij}], \quad (4.1)$$

where $u(r)$ is a long-range negative potential with a hard core of diameter a. We now define $v(r)$ as the negative part of $u(r)$ and zero inside the hard-core radius. Equation (4.1) becomes

$$\ln\Xi = \ln \sum_{N=0}^{N_0} [\exp(\beta\mu N)/N!] \int\cdots\int \prod d^3r_i \times \exp\{\tfrac{1}{2}\beta \sum [v_{ij} - v_{ij}(\text{H.C.})]\}$$
$$= \ln \sum_{N=0}^{N_0} [\exp(\beta\mu N)/N!] \int\cdots\int \prod d^3r_i \times \exp[\tfrac{1}{2}\beta \sum v_{ij}] \prod g_{ij}, \quad (4.2)$$

where $g(r)=\exp[-\beta v_{\text{H.C.}}(r)]$=zero for r less than a and unity for r greater than a. Proceeding as in the case of the lattice gas, we take the largest term in the

[7] This idea has been applied to the equation of state of dilute gases by R. Zwanzig, J. Chem. Phys. **22**, 1420 (1954).

sum over N, calling it $\bar{N}$ and then dropping the bar in the future.

$$\ln\Xi=\ln(1/N!)$$
$$+\ln\Big[\int\prod_{i=1}^{N}d^3r_i\exp(\tfrac{1}{2}\beta\sum_{i\neq j=1}^{N}v_{ij})\prod_{i<j=1}^{N}g_{ij}\Big]+N\beta\mu$$
$$=\ln W(\rho v_a)+\ln\langle\exp(\tfrac{1}{2}\beta\sum_{i\neq j}v_{ij})\rangle+N\beta\mu, \quad (4.3)$$

where $W(\rho v_a)$ is given by

$$W(\rho v_a)=(1/N!)\int\prod d^3r_i\prod_{i<j=1}^{N}g_{ij}, \quad (4.4)$$

which is just the hard-core partition function. The average of a quantity in the sense of Eq. (4.3) is defined by

$$\langle O\rangle=\int O\prod_{i<j=1}^{N}g_{ij}\prod_i d^3r_i\Big/\int\prod_{i<j=1}^{N}g_{ij}\prod d^3r_i. \quad (4.5)$$

Unfortunately, the numerator of $W(\rho v_a)$ cannot be evaluated exactly. The simplification in the lattice gas comes about because each particle can exclude only its hard-core volume which is simply the volume of the unit cell of the lattice. This is true for all positions of the remaining particles. In the real hard-core gas, two particles can exclude less than twice their individual hard-core volumes if they get too close to each other since the regions of exclusion will then overlap. Similarly, n particles can exclude less than n times their hard-core volumes and in a very complicated way. However, if we assume that $W(\rho v_a)$ is a known function (e.g., by machine calculations), we can proceed formally as with the lattice gas.

We expand the logarithm of the average in Eq. (4.3) in a semi-invariant series

$$\ln\langle\exp(\tfrac{1}{2}\beta\sum v_{ij})\rangle=\sum_{n=1}^{\infty}(\beta^n/n!)M_n(\tfrac{1}{2}\sum v_{ij}), \quad (4.6)$$

and proceed with the cluster development as in Appendix A. The derivation is given in Appendix B.

The results of the cluster expansion for the real gas differ from that of the lattice gas in two respects. In the lattice gas simple concise results were obtained by taking into account the excluded-volume problem (no two spins on the same site) by the introduction of the dashed line bonds. In the real gas, simple results expressible in terms of the two-body hard-core distribution function are obtainable only in the superposition approximation of Kirkwood[8] as applied to the hard-sphere problem. Analysis of terms of low order indicate that the error so introduced is of $O(1/z^2)$ in the critical region, but this point is not proved. In any case, the cluster expansion presented below is no longer rigorous. The second item is that, whereas in the lattice gas it was possible to sum whole classes of excluded volume graphs by introducing $M_\nu(\rho)$ at a vertex, in the real gas this is no longer possible. Thus, the results below are given before this last step is taken. In the section on the spherical model of condensation, this problem is taken up in detail for ring graphs.

The coefficient of $\beta^n/n!$ in (4.6) in superposition approximation is the sum of all irreducible graphs containing n solid lines together with all possible combinations of dashed lines (now both internal and external because of the second item in the above paragraph). However, these must not be connected sequences of dashed lines joined at a vertex at which is not also joined a solid line. Unlike the case for a lattice gas, Fig. 16 must also appear.

To each solid line associate a factor $g^{(2)}(r)v(r)$ where $g^{(2)}(r)$ is the two-body hard-core distribution function normalized according to Eq. (B15) and to each dashed line a factor $[g^{(2)}(r)-1]\equiv\tilde{f}(r)$. The value of a graph with m vertices is ρ^m times an m-fold integral over the variables $\mathbf{r}_1,\cdots,\mathbf{r}_m$ associated with the vertices. The integrand is the product of factors associated with the various bonds in the graph. The number of times a particular graph appears is a combinatorial problem which is not of interest in the present work. It may be calculated using the techniques of IV. What is useful for us at present is that a simple linked-cluster expansion exists (at least in superposition approximation) and this may be used to classify terms to $O(1/z)$ in analogy to the Ising model.

V. RESULTS OF THE THEORY OF THE REAL GAS MOLECULAR FIELD THEORY OF CONDENSATION

Following the treatment of the Ising model and the lattice gas, we first take the zeroth-order diagram as the only contribution to the pressure. We call this the molecular field because in this approximation, each particle feels the same interaction with all other particles regardless of the configuration of the system. This in effect neglects fluctuations in the local density due to the attraction. It will be exact in the limit of infinitely long, infinitely weak attractive forces. The pressure is given by

$$(1/N)\ln\Xi=\beta\rho V/N=(1/N)\ln W(\rho v_a)+\tfrac{1}{2}\rho v_a\beta\tilde{v}(0)+\beta\mu$$
$$\equiv\ln w(\rho v_a)+\tfrac{1}{2}\rho v_a\beta\tilde{v}(0)+\beta\mu, \quad (5.1)$$

where

$$\tilde{v}(0)=(1/v_a)\int v(\mathbf{r})g^{(2)}(\mathbf{r})d\mathbf{r}$$

and $\ln w(\rho v_a)=(1/N)\ln W(\rho v_a)$ is the free energy per particle for hard cores alone. $\beta\mu$ is determined from the

[8] J. G. Kirkwood, J. Chem. Phys. 3, 300 (1935).

saddle condition

$$\beta\mu=(\partial\beta F/\partial N)_{\beta,V}=-[\partial(\rho v_a \ln w(\rho v_a))/\partial\rho v_a] -\tfrac{1}{2}[\partial(\rho v_a)^2\beta\tilde{v}(0)/\partial\rho v_a] =(\partial/\partial\rho v_a)(\rho v_a \ln w)-\rho v_a\beta\tilde{v}(0) -\tfrac{1}{2}(\rho v_a)^2\partial\tilde{v}(0)/\partial\rho v_a. \quad (5.2)$$

$$\frac{\beta pV}{N}=-\frac{\partial \ln w}{\partial\rho v_a}\rho v_a-\tfrac{1}{2}\rho v_a\beta\tilde{v}(0)-\tfrac{1}{2}(\rho v_a)^2\beta\frac{\partial\tilde{v}(0)}{\partial\rho v_a} =(\beta pV/N)_{\text{H.C.}}-\tfrac{1}{2}\rho v_a\beta\tilde{v}(0) -\tfrac{1}{2}(\rho v_a)^2\partial\beta\tilde{v}(0)/\partial\rho v_a, \quad (5.3)$$

where the subscript H.C. denotes a quantity evaluated for hard cores alone. The critical temperature is determined by setting the isothermal compressibility equal to infinity. This gives the equation

$$V(\partial p/\partial V)_{N,T}=-\rho(\partial p/\partial\rho)_T=0, \quad (5.4)$$

the solutions of which are $\rho=0$ which is uninteresting, and $(\partial p/\partial\rho)_T=0$ which we rewrite as

$$0=-\beta/\rho v_a(\partial p/\partial\rho v_a)_T =2(\partial \ln w/\partial\rho v_a)+\rho v_a[\partial^2 \ln w/\partial(\rho v_a)^2]+\beta\tilde{v}(0) +2\rho v_a\beta[\partial\tilde{v}(0)/\partial\rho v_a]+\tfrac{1}{2}(\rho v_a)^2\beta[\partial^2\tilde{v}(0)/\partial(\rho v_a)^2]. \quad (5.5)$$

The function $p(\rho,\beta)$ as written in Eq. (5.1) will show loops as a function of ρ for $\beta>\beta_c$ since it is analytic, whereas the true pressure consists of three analytic parts for $\beta>\beta_c$. This, of course, is due to the fact that the pressure, as written, is not valid in the region inside the loops for the same reason in the Ising case. Equation (5.5) will necessarily show spurious zeros (minima and maxima of the loops) when the temperature is below the critical value. Hence, to determine the critical temperature and density, we must take the smallest value of β for which it is possible to find a root of Eq. (5.5). We get

$$0=\partial\beta/\partial\rho v_a=-\{\tilde{v}(0)+2\rho v_a[\partial\tilde{v}(0)/\partial\rho v_a] +\tfrac{1}{2}(\rho v_a)^2[\partial^2\tilde{v}(0)/\partial(\rho v_a)^2]\}^{-1}\partial^3(\rho v_a \ln w)/\partial(\rho v_a)^3 +\{3(\partial\tilde{v}(0)/\partial\rho v_a)+3\rho v_a[\partial^2\tilde{v}(0)/\partial(\rho v_a)^2] +\tfrac{1}{2}(\rho v_a)^2[\partial^3\tilde{v}(0)/\partial(\rho v_a)^3]\}\{\tilde{v}(0)+2\rho v_a[\partial\tilde{v}(0)/\partial\rho v_a] +\tfrac{1}{2}(\rho v_a)^2[\partial^2\tilde{v}(0)/\partial(\rho v_a)^2]\}^{-2}\partial^2(\rho v_a \ln w)/\partial(\rho v_a)^2. \quad (5.6)$$

In order to solve Eq. (5.6) for ρ_c, it is necessary to know $\ln w$ and $\tilde{v}(0)$ as functions of ρ. As we shall see, the critical density (ρv_a) is in the neighborhood of $\frac{1}{4}$ so that good values are given by the density (virial) expansions of the pressure and the pair correlation function from which we can determine the density expansions for $\ln w$ and $\tilde{v}(0)$. Using the virial coefficients for the pressure and the tabulated values of the coefficient of $(\rho v_a)^2$ contributing to $g^{(2)}(r)$,[9] we find

$$(\beta pV/N)_{\text{H.C.}} =1+\beta_1\rho v_a+\beta_2(\rho v_a)^2+\beta_3(\rho v_a)^3+\beta_4(\rho v_a)^4+\cdots \quad (5.7)$$

$$=-\rho v_a(\partial \ln w/\partial\rho v_a), \quad (5.8)$$

$$\tilde{v}(0)=\alpha_0[1+\alpha_1\rho v_a+\alpha_2(\rho v_a)^2+\cdots], \quad (5.9)$$

where

$$\beta_1=2.9615,\ \beta_2=5.4816,\ \beta_3=7.4519,\ \beta_4=8.846. \quad (5.10)$$

In order to compare the answers obtained from the molecular field approximation with previous work on the subject and also with experiment, we take the negative part of the Lennard-Jones potential,[10] $4\epsilon[(a/r)^{12}-(a/r)^6]$ for the attractive tail; $v(r)=0$ for $r<a$. We find

$$\alpha_0=15.797\epsilon,\quad \alpha_1=0.69241,\quad \alpha_2=-0.12439. \quad (5.11)$$

The last coefficient was obtained by numerical integration. Equation (5.6) becomes

$$1/(\rho v_a)^2+6\alpha_1/\rho v_a-(3\beta_2-16\alpha_2-6\beta_1\alpha_1) -(8\beta_3-24\beta_1\alpha_2)\rho v_a-(15\beta_4+12\beta_3\alpha_1-24\beta_2\alpha_2)(\rho v_a)^2 -(30\beta_4\alpha_1-16\beta_3\alpha_2)(\rho v_a)^3+O(\rho v_a)^4=0. \quad (5.12)$$

Putting in the values for the coefficients, we find

$$1/(\rho v_a)^2+4.155/(\rho v_a)-6.131-68.46\rho v_a -211.0(\rho v_a)^2-198.6(\rho v_a)^3+O(\rho v_a)^4=0. \quad (5.13)$$

Since the terms with positive sign in Eq. (4.13) decrease monotonically for positive ρv_a and the terms with negative sign increase monotonically for positive ρv_a, there is only one positive real root which is $\rho_c v_a=0.233$. Assuming that all the truncated series are essentially geometric, we estimate the error in the above result to be about 3%.

We now use the value of $\rho_c v_a$ in Eq. (5.5) to obtain $\beta_c\epsilon$ and in Eq. (5.3) to determine $\beta_c p_c v_c$. The values are listed in Table I together with those obtained by Kirkwood, Lewinson, and Alder[11] for the modified

TABLE I. Comparison of some dimensionless constants in the theory of condensation evaluated by three methods.

	v_c/a^3	$[\beta_c\epsilon]^{-1}$	$\beta_c p_c v_c$
Expt.	3.09	1.28	0.292
K–L–A	2.59	1.43	0.358
Molecular field theory	3.04	1.42	0.418

[9] See B. R. A. Nijboer and L. Van Hove, Phys. Rev. **85**, 777 (1952).

[10] In the above calculations we have used the so-called Lennard-Jones (6–12) potential where the numbers in parentheses denote the exponents of the attractive and repulsive parts. See, for example, J. O. Hirschfelder, C. F. Curtiss, and R. B. Bird, *Molecular Theory of Gases and Liquids* (John Wiley & Sons. Inc., New York, 1954), p. 162.

[11] J. G. Kirkwood, V. A. Lewinson, and B. J. Alder, J. Chem. Phys. **20**, 929 (1952). This kind of theory, as usually presented, gives little qualitative understanding of the condensation phenomenon but is based on the observations that the pressure-volume isotherms as calculated turn out to have loops. In the present theory, the advantage is that the qualitative physics of the phenomenon is "fed" into the theory at the outset.

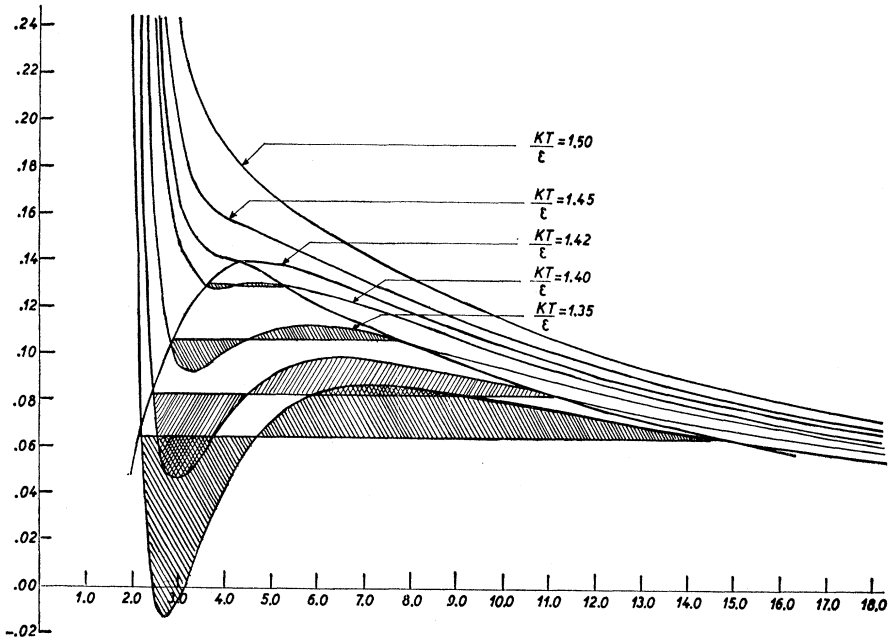

FIG. 2. Pressure-volume isotherms of the real gas in molecular field approximation. The abscissa is (v/v_a).

Lennard-Jones potential (Lennard-Jones potential with hard core) and experimental results.[12] The theory of Kirkwood *et al.* is based on recursion relations of distribution functions and the Kirkwood superposition approximation.

The discrepancy of the molecular field value of $\beta_c p_c v_c$ with the experimentally determined value is due to the very strong dependence of this quantity on the value of the critical temperature. $\beta_c p_c v_c$ is of the form $A(\rho_c v_a) - \rho_c B(\rho_c v_a)$, where A and B are themselves not very sensitive to $\rho_c v_a$ and β_c. If the true T_c were only 10% lower than the molecular field value, the value of $\beta_c \rho_c v_c$ would be reduced by about 40% which brings it into line with experiment. Note that this correction is to be expected. On the basis of Ising model calculations, the Curie point as calculated in molecular field theory is indeed about 10% too high for near-neighbor interactions.

In Fig. 2, we have plotted isotherms in the $p-v$ plane for various values of kT/ϵ. Below the critical temperature, the isotherms show the familiar loops which are inherent in a canonical ensemble calculation when the attractive part of the potential has infinite range (molecular field). It must be emphasized, however, that the replacement of the loops by a straight line cutting off equal areas (Maxwell construction) is not an *ad hoc* procedure but is actually dictated by the theory itself. In the grand ensemble, the loops are immediately eliminated because steepest descents have been used to evaluate the integral (sum) over the number of particles and the formal equations are not valid for values of the density inside the loops. The reasoning here is the same as for the Ising model molecular field theory in Sec. II. This agrees with the theorem that $\partial p/\partial v$ is negative for a grand ensemble calculation whether the canonical ensemble partition function used is correct or not.[13]

In general, we may conclude that the molecular field theory using the hard-core metric gives all the qualitative features of condensation as well as surprisingly good quantitative features. We clearly have a successful zeroth approximation to the phenomenon together with qualitative understanding. The entropy is essentially that of the hard-core gas and the energy that of the tail. At low temperature (below T_c), the latter wins out and condensation occurs.

Spherical Model of Condensation

We have seen that in the theory of the lattice gas it is possible to take account of microscopic fluctuations in the density by summing a set of ring graphs (spherical model). In the case of the real gas, we shall show that this theory again leads to fluctuations of the Ornstein-Zernicke type.[3] The motivation will be, as in the Ising case, to obtain the first-order correction (coefficient of v_a/v_s in the pressure) to the molecular field theory. We make the tacit assumption that such an expansion of the pressure in powers of v_a/v_s is possible and yields physically consistent results when truncated at any order. It is unfortunate that the spherical model graphs summation at this point has not led to such simple results as for the lattice gas. Nevertheless, we include it here to illustrate how our cluster method works.

[12] The experimental results quoted in the text are the mean value for Ne, N_2, Ar, and CH_4 taken from T. L. Hill, *Statistical Mechanics* (McGraw-Hill Book Company, Inc., New York, 1956), p. 232.

[13] See, for example, T. L. Hill, reference 12, p. 166.

If it were not for the following complication, we could transcribe the results for the spherical model in the Ising case as we did for the lattice gas. Consider the diagrams of Fig. 23 in Appendix C. In the case of the lattice gas, they add up to the value shown in Fig. 24. For the real gas, the three diagrams of Fig. 23 are not equivalent in absolute value. We, therefore, make the approximation that they add up to the single diagram as in Fig. 24 for the lattice gas. It is virtually impossible to estimate with any accuracy the error involved in this approximation but it appears reasonable if the range of the potential is large compared with the size of the hard core (large z). This is evident from Fig. 23 where we see that vertices 1, 3, and 5 are relatively close together compared with the other vertices whether there are two dotted lines or three. Note that this approximation does not depend on the density of the system but rather on v_a/v_s since ρ enters only as a factor multiplying each diagram.

We can now eliminate the external dashed lines from ring diagrams containing internal dashed lines. We denote, as with the lattice gas, the sum of all external dotted line ring graphs (with or without internal dashed lines) by a skeleton ring graph in which each "vertex" stands for $\rho v_a[\delta(\mathbf{r}_i-\mathbf{r}_i')-\rho v_a\tilde{f}(\mathbf{r}_i-\mathbf{r}_i')]=M_{ii'}{}^{(2)}$. The term "vertex" is used to denote two points, r_i and r_i' connected by an $M_{ii'}{}^{(2)}(\mathbf{r}_i-\mathbf{r}_{i'})$ bond. We can now sum the set of all ring graphs with noncrossing internal dashed lines as before in the Ising model. We look at the pressure first.

$$\beta pv=\ln w(\rho v_a)+\tfrac{1}{2}\beta\tilde{v}(0)\rho v_a+(1/2N)\sum_{n=3}^{\infty}\left\{\int(\beta^n/n)[z_{12'}M_{22'}{}^{(2)}z_{2'3}\cdots z_{n1'}M_{1'1}{}^{(2)}]\prod_{i=1}^{n}d\mathbf{r}_i d\mathbf{r}_{i'}\right\}$$

$$+(\beta^2/4N)\int d\mathbf{r}_1 d\mathbf{r}_{1'} d\mathbf{r}_2 d\mathbf{r}_{2'}\, v_{12'}M_{2'2}{}^{(2)}v_{21'}M_{1'1}{}^{(2)}+(\beta^2/4N)\int d\mathbf{r}_1 d\mathbf{r}_{1'} d\mathbf{r}_2 d\mathbf{r}_{2'}$$

$$\times\epsilon(\mathbf{r}_1-\mathbf{r}_{2'})M_{2'2}{}^{(2)}\epsilon(\mathbf{r}_2-\mathbf{r}_{1'})M_{1'1}{}^{(2)}+\beta\mu, \quad (5.14)$$

where

$$z(\mathbf{r}_i-\mathbf{r}_j)=v(\mathbf{r}_i-\mathbf{r}_j)g^{(2)}(\mathbf{r}_i-\mathbf{r}_j)-\epsilon(\mathbf{r}_j-\mathbf{r}_j). \quad (5.15)$$

The saddle parameter $\epsilon(\mathbf{r}_j-\mathbf{r}_j)$ is now a function of the positions of the vertices since $\tilde{f}(\mathbf{r}_i-\mathbf{r}_j)$ is not a delta function as in the lattice gas.

In the expression for the pressure, the first two terms

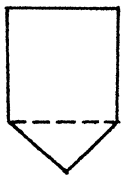

FIG. 3. Ring graph which is recounted by the third term of Eq. (5.14).

are the hard sphere entropy and the molecular field. The third term is the sum of all rings starting with the triangle and with the v bonds replaced by z bonds. The fourth term is simply the single second-order diagram in the cluster expansion. This would appear to give the sum of all rings with noncrossing internal dashed lines but graphs of the type of Fig. 3 are counted twice. This is because we can look at the bonds on either side of the dotted line as contained in the saddle parameter. Other graphs of the type of Fig. 3 are also overcounted by various amounts. The fifth term in Eq. (5.14) subtracts just those terms which are overcounted. The last term is the chemical potential. Using Fourier transforms, the pressure becomes

$$\begin{aligned}\beta pv=&\ln w(\rho v_a)+\tfrac{1}{2}\rho v_a\beta\tilde{v}(0)\\&-(1/2N)\sum_{q\neq 0}\ln[1-\beta M^{(2)}(\mathbf{q})z(\mathbf{q})]\\&+(1/2N)\sum_{q\neq 0}\Delta(\mathbf{q})M^{(2)}(\mathbf{q})\\&+(1/2N)\sum_{q\neq 0}\beta^2\tilde{v}(\mathbf{q})\Delta(\mathbf{q})[M^{(2)}(\mathbf{q})]^2\\&+(\beta^2/4N)\sum_{q\neq 0}[\Delta(\mathbf{q})\epsilon(\mathbf{q})-\Delta^2(\mathbf{q})][M^{(2)}(\mathbf{q})]^2\\&-(\beta/2N)\sum_{\mathbf{q}\neq 0}\tilde{v}(\mathbf{q})M^{(2)}(\mathbf{q})+\beta\mu. \quad (5.16)\end{aligned}$$

Here $\epsilon(\mathbf{q})$ is the Fourier transform of the saddle parameter and $\Delta(\mathbf{q})$ is the Fourier transform of $\epsilon_{ij}\tilde{f}_{ij}$ which is $\sum_{q'}\tilde{f}(\mathbf{q}-\mathbf{q}')\epsilon(\mathbf{q}')$. Equation (5.16) reduces to Eq. (3.18) for the lattice gas when it is remembered that $f(\mathbf{q})=1$, so that $(1/N)\sum\epsilon(\mathbf{q})=\Delta(\mathbf{q})=\delta$. Instead of looking at the energy as in the Ising model, we determine the sum rule by calculating $\epsilon(\mathbf{q})$ directly. ϵ_{ij} is the sum of all irreducible ring graphs attached to two points. This is shown in Fig. 4. Replacing each v bond by a z bond counts all graphs correctly. The reason is that two points are fixed and there is no ambiguity about which side of a dotted line to consider as contributing to a z bond. We thus get for ϵ_{ij}

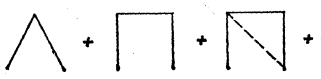

FIG. 4. Diagram contributing to ϵ_{ij}.

$$\epsilon(\mathbf{r}_1-\mathbf{r}_2)=\sum_{n=3}^{\infty}\int\prod_{i=3}^{n}d\mathbf{r}_i d\mathbf{r}_{i'}z_{13'}M_{3'3}{}^{(2)}\cdots M_{n'n}{}^{(2)}z_{n2}. \quad (5.17)$$

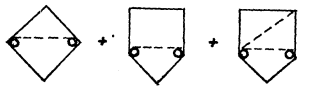

FIG. 5. Correction diagrams for the pressure.

The Fourier transform of Eq. (5.17) is

$$\epsilon(\mathbf{q})=\frac{z(\mathbf{q})}{1-\beta z(\mathbf{q})M^{(2)}(\mathbf{q})}-\tilde{v}(\mathbf{q})+\Delta(\mathbf{q}). \quad (5.18)$$

From Eq. (5.18), it follows that the pressure is stationary with respect to $\Delta(\mathbf{q})$ regarded as an independent variable. We have

$$\begin{aligned}2\partial\beta pv/\partial\Delta(\mathbf{q})&=-\frac{-\beta M^{(2)}(\mathbf{q})}{1-\beta z(\mathbf{q})M^{(2)}(\mathbf{q})}+\beta M^{(2)}(\mathbf{q})+\beta v(\mathbf{q})[M^{(2)}(\mathbf{q})]^2\\&\quad-\beta^2\Delta(\mathbf{q})[M^{(2)}(\mathbf{q})]^2+\tfrac{1}{2}[\partial/\partial\Delta(\mathbf{q})]\\&\quad\times\sum_{q\neq 0}\beta^2\Delta(q)\epsilon(q)[M_2(\mathbf{q})]^2. \quad (5.19)\end{aligned}$$

The last term of Eq. (5.19) appears to give trouble. However, it must be noted that the sum in the last term must be read symbolically in the following sense. Since the term $[M_2(\mathbf{q})]^2$ appears in the sum, it causes an asymmetry since it puts $\epsilon(\mathbf{q})$ and $\Delta(\mathbf{q})$ on an equal basis. This is shown more clearly when we write the sum as $\sum_{\mathbf{q},\mathbf{q}'}\epsilon(\mathbf{q})\tilde{f}(\mathbf{q}-\mathbf{q}')\epsilon(\mathbf{q}')[M^{(2)}(\mathbf{q})]^2$. What should be subtracted in order to correct for overcounting in the expression for the pressure is the sum of the diagrams of Fig. 5 where the circles denote $M_{ii'}{}^{(2)}$. The sum, on the other hand, denotes the graphs of Fig. 5 but with half of them having the dashed lines on the other side of the circles as shown in Fig. 6. When this correct procedure is done, it is seen that the derivative with respect to $\Delta(\mathbf{q})$ is actually $2\epsilon(\mathbf{q})[M^{(2)}(\mathbf{q})]^2$ since the argument of $M^{(2)}$ changes from q to q' depending on which ϵ is referred to. With the help of the foregoing argument, Eq. (5.19) becomes

$$\begin{aligned}2\partial\beta pv/\partial\Delta(\mathbf{q})&=-\frac{\beta^2 z(\mathbf{q})[M^{(2)}(\mathbf{q})]^2}{1-\beta z(\mathbf{q})M^{(2)}(\mathbf{q})}+\beta^2\tilde{v}(\mathbf{q})[M^{(2)}(\mathbf{q})]^2\\&\quad-\beta^2\Delta(\mathbf{q})[M^{(2)}(\mathbf{q})]^2+\beta^2\epsilon(\mathbf{q})[M^{(2)}(\mathbf{q})]^2. \quad (5.20)\end{aligned}$$

Comparing Eq. (5.20) with (5.18), we see that the equation

$$\partial\beta pV/\partial\Delta(\mathbf{q})=0 \quad (5.21)$$

is shown below to be equivalent to a sum rule reminiscent of the spherical model.

To see the connection between the sum rule and fluctuations, we look at the microscopic density. This is defined by

$$\rho(\mathbf{r})=\sum_{i=1}^{N}\delta(\mathbf{r}-\mathbf{r}_i), \quad (5.22)$$

which is a quantity analogous to ϵ_i of the lattice gas. The Fourier transform $\rho_\mathbf{q}$ is defined as

$$\rho_\mathbf{q}=(\rho^{1/2}/N^{1/2})\sum\exp(i\mathbf{q}\cdot\mathbf{r}_i), \quad (5.23)$$

$$\sum|\rho_\mathbf{q}|^2=(\rho/N)\sum_{i,j}\sum_{\mathbf{q}}\exp[i\mathbf{q}\cdot(\mathbf{r}_i-\mathbf{r}_j)]. \quad (5.24)$$

The right-hand term is zero when $i\neq j$ since for hard cores, $r_i\neq r_j$ when $i\neq j$. This is not true if the repulsive part of the potential is not infinite inside a finite volume (hard core), Eq. (5.24) then becomes for hard cores

$$\sum_\mathbf{q}|\rho_\mathbf{q}|^2=\sum_\mathbf{q}\rho, \quad (5.25)$$

or

$$\sum_\mathbf{q}[|\rho_\mathbf{q}|^2-\rho]=0. \quad (5.26)$$

This is the spherical condition which corresponds to Eq. (3.21) for the lattice gas. Using the above expansion, we can evaluate $\langle|\rho_\mathbf{q}|^2\rangle$ from the sum of all spherical model graphs attached to two fixed points, i and j. From (5.24) we see that this latter is just the Fourier transform of the sum of all spherical model graphs attached to this two points. We thus have

$$\begin{aligned}\langle|\rho_\mathbf{q}|^2\rangle&=\rho-\rho^2v_a\tilde{f}(\mathbf{q})+\frac{1}{N_0}\sum_{n=3}^{\infty}\beta^n\sum_{q'}[z(\mathbf{q}')]^{n-1}[M^{(2)}(\mathbf{q})]^n\\&\quad+(1/N_0)\beta\sum_{\mathbf{q}'}v(\mathbf{q}')[M^{(2)}(\mathbf{q})]^2g^{(2)}(\mathbf{q}-\mathbf{q}')\\&=\rho-\rho^2v_a\tilde{f}(\mathbf{q})+\frac{1}{N_0}\sum_{q'}\left\{\frac{M^{(2)}(\mathbf{q}')}{1-\beta M^{(2)}(\mathbf{q}')z(\mathbf{q}')}\right.\\&\quad\left.-M^{(2)}(\mathbf{q}')+\beta\Delta(\mathbf{q}')[M^{(2)}(\mathbf{q}')]^2\right\}g^{(2)}(\mathbf{q}-\mathbf{q}').\end{aligned} \quad (5.27)$$

Summing over q, we obtain the sum rule in the form

$$\sum_{q\neq 0}[\langle|\rho_\mathbf{q}|^2\rangle-(1/v_a)M^{(2)}(\mathbf{q})]=0, \quad (5.28)$$

since $\sum g^{(2)}(\mathbf{q})=0$. It is easy to see what Eq. (5.27) reduces to for the lattice gas. In this case

$$g^{(2)}(\mathbf{r}_i-\mathbf{r}_j)=1-\delta_{\mathbf{r}_i\mathbf{r}_j}, \quad (5.29)$$

$$g^{(2)}(\mathbf{q})=N_0\delta_{0\mathbf{q}}-1. \quad (5.30)$$

Also

$$\Delta(\mathbf{q})=\sum\epsilon(\mathbf{q}')g(\mathbf{q}-\mathbf{q}')=\epsilon, \quad (5.31)$$

$$M^{(2)}(\mathbf{q})=\rho(1-\rho), \quad (5.32)$$

so that Eq. (5.27) becomes

$$\langle|\epsilon_\mathbf{q}|^2\rangle=\rho(1-\rho)/[1-\beta\rho(1-\rho)z(\mathbf{q})], \quad (5.33)$$

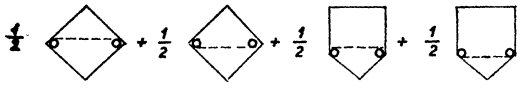

FIG. 6. Diagrams subtraced in Eq. (5.10) to correct for overcounting.

where the lattice gas sum rule, Eq. (3.19), was used. Equation (5.33) is equivalent to Eq. (3.22).

To see what $\langle|\epsilon_q|^2\rangle$ looks like in the lattice gas for small q near the critical temperature, we expand $v(\mathbf{q})$ as a function of q.

$$v(\mathbf{q})=v(0)[1-\alpha q^2], \tag{5.34}$$

where α is $O(z)$. Putting this into Eq. (5.34) we find for $T\sim T_c$

$$\langle|\epsilon_q|^2\rangle=\rho(1-\rho)/\{1-\beta\rho(1-\rho)[v(0)(1-\alpha q^2)-\epsilon]\}$$
$$=\frac{1/4}{1-(\beta/4)[4kT_c-\alpha q^2 v(0)]}=\frac{\frac{1}{4}(T/\gamma T_c)}{\lambda^2+q^2}, \tag{5.35}$$

where $\gamma=v(0)/z(0)$ and $\lambda=\gamma^{-1/2}(T/T_c-1)^{1/2}$. Equation (5.36) holds for $\rho=\rho_c=\frac{1}{2}$. This shows how the correlation length, λ^{-1} becomes infinite near the critical temperature for $\rho=\rho_c$.

By writing

$$g^{(2)}(q)=N_0\delta_{0q}-\tilde{f}(\mathbf{q}) \tag{5.36}$$

for the real gas, we find a form similar to Eq. (5.36). For small q, we have

$$\tilde{f}(\mathbf{q})\cong\tilde{f}(\mathbf{q}=0)+\eta q^2, \tag{5.37}$$

$$g^{(2)}(\mathbf{q})\cong N_0\delta_{0q}-\tilde{f}(\mathbf{q}=0)-\eta q^2, \tag{5.38}$$

$$M^{(2)}(\mathbf{q})\cong\rho v_a\{1-[\tilde{f}(\mathbf{q}=0)+\eta q^2]\rho v_a\}, \tag{5.39}$$

where $f(\mathbf{q}=0)$ stands for $\lim_{\mathbf{q}\to 0}f(\mathbf{q})$. Note that $f(\mathbf{q}=0)$ is not equal to $f(0)$ $(=0)$ as defined in Eq. (4.21). This is a consequence of the normalization we need for $g^{(n)}(\mathbf{r}_1,\cdots,\mathbf{r}_n)$ which is the most convenient for deriving the cluster expansion. $f(\mathbf{q}=0)$ is easily evaluated by noting that[13]

$$\tilde{f}(\mathbf{r})\underset{r\to\infty}{\to}(1-\rho kT\kappa_{\text{H.S.}})/N. \tag{5.40}$$

Then

$$\tilde{f}(0)=\tilde{f}(\mathbf{q}=0)-(1/\rho-kT\kappa_{\text{H.S.}})=0, \tag{5.41}$$

or

$$\tilde{f}(\mathbf{q}=0)=1/\rho-kT\kappa_{\text{H.S.}}, \tag{5.42}$$

where $\kappa_{\text{H.S.}}$ is the isothermal compressibility for hard cores alone. If we had chosen the grand ensemble normalization for $g^{(n)}(\mathbf{r}_1\cdots,\mathbf{r}_n)$ we would have obtained

$$\tilde{f}(0)=\tilde{f}(\mathbf{q}=0)=1/\rho-kT\kappa_{\text{H.S.}}. \tag{5.43}$$

It is important to note that the quantity with physical meaning is $\tilde{f}(q=0)$ and not $\tilde{f}(0)$ which is arbitrary to within an additive Kronecker delta.

It should also be noted that for the lattice gas,

$$\kappa_{\text{L.G.}}=\beta(1-\rho)/\rho, \tag{5.44}$$

so that $\tilde{f}(q=0)=1$ as it should.

From Eq. (5.27), we see that the principal contribution to $\langle|\rho_q|^2\rangle$ is

$$\langle|\rho_q|^2\rangle\cong M^{(2)}(\mathbf{q})/[1-\beta M^{(2)}(\mathbf{q})z(\mathbf{q})]. \tag{5.45}$$

From the denominator of Eq. (5.45) we see that the critical temperature is given by

$$M^{(2)}(0)z(0)=\rho v_a[1-\tilde{f}(\mathbf{q}=0)\rho v_a]z(0)=1, \tag{5.46}$$

and since the form of $v(q)$ is given by Eq. (5.34), the form of $\langle|\rho_q|^2\rangle$ will be given by Eq. (5.35). However, because of the complexity of the spherical model in the present case, we cannot show that the value of the critical temperature as determined by infinite compressibility is the same as Eq. (5.46).

We have shown that the form given by Eq. (5.35) is a reasonable conjecture but at present we do not have a rigorous proof for this; these results are of the Ornstein-Zernicke type.

Note also that in analogy to the lattice gas the expansion for $\langle|\rho_q|^2\rangle$ for small q is in powers of ρv_a $\times[1-\tilde{f}(\mathbf{q}=0)\rho v_a]$ where $\tilde{f}(q=0)=1-\rho kT\kappa_{\text{H.S.}}$. In the liquid range, $\kappa_{\text{H.S.}}\to 0$ and one recovers the expansion coefficients similar to $\rho v_a[1-\rho v_a]$ of the lattice gas. In other words, whereas our expansion in the gas phase is an expansion in density of particles, in the liquid it is an expansion something like the number of holes. In the critical region the parameter is mixed. The reason for the unsymmetric isotherms $(\rho v_a\neq\frac{1}{2})$ is that the real hard-core gas has interesting variation of compressibility with density.

The isothermal compressibility is given by the fluctuation in the microscopic density. We have

$$\frac{\langle\rho^2(0)\rangle-\langle\rho(0)\rangle^2}{\langle\rho(0)\rangle^2}=\frac{kT\kappa}{V}. \tag{5.47}$$

κ can be calculated directly from its definition using the spherical model value for the pressure. Also, the relative fluctuation in Eq. (5.47) can be calculated directly. From the analysis of the spherical model in the Ising case, it will be seen that the two quantities will not be equal as they should from Eq. (5.47) although they will become infinite at the same value of T. We, therefore, have the same inconsistency which obtains in the spherical model of the Ising model. For this reason we postpone further analysis of the present treatment until some of these difficulties are cleared up.

VI. CONCLUSION

We have seen that it is possible to derive a cluster expansion for the lattice gas without recourse to (although the formalism is the same as that of) the Ising model. Using this derivation plus the fact that the quantity $\rho(1-\rho)$ occurs in the expansion of the pressure of the lattice gas, we conjecture that the hard core plays a predominant role in the theory of condensation since it allows a formulation of the equation of state of the gaseous and liquid states together. To this end, we have developed a cluster expansion for a classical system of particles with hard cores and weakly attracting long tails with the hard core treated exactly as it

is for the lattice gas. We have seen that in the limit of infinitely long and infinitesimally weak attractive tails (molecular field), we obtain a theory of condensation which has the same essential features as the Weiss theory of ferromagnetism. Noting the partial success of the spherical model of ferromagnetism, we attempt an analogy for the real gas and find essentially the same results although it is very difficult to perform any numerical calculations. We do, however, gain some insight into the mechanism of condensation since we obtain a series in the density which diverges for a critical value of the density when $T<T_c$ and converges again after condensation is completed because of the occurrence of factors of the form $\rho(1-\rho)$. We have shown that by a reformulation of Mayer's original cluster expansion using a hard-core metric, it is possible to obtain a qualitative understanding of the mechanism of condensation and to calculate quantitative results from a simple approximation to the rigorous theory. It is hoped that a consistent first-order correction to this molecular field theory will be obtained by the possible summation of all convolution graphs (nodal expansion)[14] in the present cluster expansion.

Note added in proof. It has been kindly pointed out to us by Professor A. Siegert that the molecular field approximation is very close to the van der Waals approximation to the equation of state. In particular, if $W(\rho v_a)$ in Eq. (5.1) is approximated by $(V/N-v_a)^N$ and the dependence of $g^{(2)}(r)$ on ρ is neglected, the resulting theory is that of van der Waals. The parameter a is $\tilde{v}(0)$ and the parameter b is (v_a). It is remarkable that the two corrections included in our version of the theory bring the van der Waals theory into such close accord with experiment.

It may be pointed out here that this whole development is completely rigorous for a one-dimensional system of hard bars and an infinite-range potential whose integral over the whole real axis exists [and is called $v(0)$]. In this case the van der Waals equation of state is rigorous. Of course, in one dimension, condensation only occurs for infinite-range forces.

Note added in proof. If instead of summing spherical model rings, one sums simple rings one finds

$$\langle|\rho_q|^2\rangle=\frac{\langle|\rho_q|^2\rangle_{\text{H.S.}}}{1-\beta\rho v(\mathbf{q})\langle|\rho_q|^2\rangle_{\text{H.S.}}},$$

where

$$\langle|\rho_q|^2\rangle_{\text{H.S.}}=1-\rho\int\tilde{f}(\mathbf{r})e^{iq\cdot r}d\mathbf{r}.$$

In particular,

$$\lim_{q\to 0}\langle|\rho_q|^2\rangle_{\text{H.S.}}=\rho kTK_{\text{H.S.}}.$$

The critical point is then where $\rho^2K_{\text{H.S.}}v(0)=1$. This is the same as the critical temperature obtained from Eqs. (5.4) and (5.5) if one neglects the density dependence of $g^{(2)}(r)$ in $\tilde{v}(0)$. For application of this result to the theory of freezing see a forthcoming publication of R. Brout, Physica (to be published).

APPENDIX A

Our point of departure is the expansion Eq. (3.10).[15] We first recall the fundamental theorem of semi-invariants. Let $M_n^{(x)}$, $M_n^{(y)}$ be the semi-invariants generated by x and y, respectively. Then

$$M_n^{(x+y)}=M_n^{(x)}+M_n^{(y)}, \tag{A1}$$

x, y independent.

To get an idea what the expansion (3.10) looks like, we write out the first two semi-invariants explicitly. The average is written in the following way. Since the u's are functions of the positions, $\mathbf{r}$, of the particles on the lattice sites, we write them as $u_{ij}=u_{r_ir_j}$. Then the average becomes

$$\langle u_{r_ir_j}\rangle=\sum_{r_1r_2\cdots r_N=1}^{N_0}u_{r_1r_2}\prod_{i<j=1}^{N}g_{r_ir_j}\Big/\Big(\sum_{r_1r_2\cdots r_N}^{N_0}\prod_{i<j}^{N}g_{r_ir_j}\Big), \tag{A2}$$

where $g_{r_ir_j}=1-\delta_{r_ir_j}$. The purpose of the g's is to take account of the hard core by preventing two particles from occupying the same lattice site. That Eq. (A2) is equivalent to Eq. (3.9) is evident when it is observed that the numerator in Eq. (A2) is equivalent to the sum on configurations without permutations and the denominator is $W(\rho)$. The denominator in Eq. (3.12) can be written

$$\begin{aligned}\sum_{r_1\cdots r_N=1}^{N_0}\prod_{i<j=1}^{N}g_{r_ir_j}&=(N_0-N+1)\sum_{r_1\cdots r_{N-1}}^{N_0}\prod_{i<j=1}^{N-1}g_{r_ir_j}\\&=(N_0-N+1)\cdots(N_0-n)\sum_{r_1\cdots r_n}^{N_0}\prod_{i<j=1}^{n}g_{r_ir_j}\end{aligned} \tag{A3}$$

for $2\leq n<N$. If we take $n=2$ in Eq. (3.13), then the common factors in the numerator and denominator cancel and we are left with

$$\langle u_{r_1r_2}\rangle=\frac{\sum_{r_1r_2}^{N_0}u_{r_1r_2}g_{r_1r_2}}{\sum_{r_1r_2}g_{r_1r_2}}=\frac{N_0}{N_0(N_0-1)}u(0), \tag{A4}$$

[14] See E. Meeron, Phys. Fluids **1**, 139 (1958).

[15] Many of the graphical ideas introduced here such as reducibility are assumed known to the reader from standard works on statistical mechanics [e.g., T. L. Hill (reference 12)]. The general pattern of development is similar to the works of reference 1 with which the reader is assumed to be familiar.

where $u(\mathbf{q})$ is defined by

$$u(\mathbf{q})=(1/N_0)\sum_{r_i\neq rj=1}^{N_0} u_{r_ir_j}\exp[i\mathbf{q}\cdot(\mathbf{r}_i-\mathbf{r}_j)]. \quad \text{(A5)}$$

The first semi-invariant is given by

$$M_1=\tfrac{1}{2}\sum_{i\neq j=1}^{N}\langle u_{r_ir_j}\rangle=\tfrac{1}{2}[N(N-1)/(N_0-1)]u(0)$$
$$=\tfrac{1}{2}N_0u(0)\rho^2+O(1). \quad \text{(A6)}$$

For the second semi-invariant, we have

$$M_2=\tfrac{1}{4}[\langle\sum_{i\neq j,k\neq l}u_{r_ir_j}u_{r_kr_l}\rangle-\langle\sum_{i\neq j}u_{r_ir_j}\rangle\langle\sum_{k\neq l}u_{r_kr_l}\rangle]$$
$$=\tfrac{1}{4}\sum_{i\neq j\neq k\neq l}[\langle u_{r_ir_j}u_{r_kr_l}\rangle-\langle u_{r_ir_j}\rangle\langle u_{r_kr_l}\rangle]+\sum_{i\neq j\neq k}[\langle u_{r_ir_j}u_{r_jr_k}\rangle-\langle u_{r_ir_j}\rangle\langle u_{r_jr_k}\rangle]+\tfrac{1}{2}\sum_{i\neq j}[\langle u_{r_ir_j}{}^2\rangle-\langle u_{r_ir_j}\rangle^2]. \quad \text{(A7)}$$

The motivation for writing Eq. (A7) will be seen when we consider the individual terms. We start with the first.

$$\langle u_{r_ir_j}u_{r_kr_l}\rangle-\langle u_{r_ir_j}\rangle\langle u_{r_kr_l}\rangle=\frac{\sum u_{r_1r_2}u_{r_3r_4}\prod_{i<j=1}^{4}g_{r_ir_j}}{\sum\prod_{i<j=1}^{4}g_{r_ir_j}}-\frac{\sum u_{r_1r_2}g_{r_1r_2}}{\sum g_{r_1r_2}}\frac{\sum u_{r_3r_4}g_{r_3r_4}}{\sum g_{r_3r_4}}$$

$$=\frac{\sum_{r_1'\cdots r_4'}\sum_{r_1\cdots r_4}u_{r_1r_2}u_{r_3r_4}[\prod_{i<j=1}^{4}(g_{r_ir_j})g_{r_1'r_2'}g_{r_3'r_4'}-g_{r_1r_2}g_{r_3r_4}\prod_{i<j=1}^{4}(g_{r_i'r_j'})]}{\sum\prod_{i<j=1}^{4}(g_{r_ir_j})g_{r_1'r_2'}g_{r_3'r_4'}}, \quad \text{(A8)}$$

where we have used the reduction

$$\langle F(\mathbf{r}_1,\mathbf{r}_2,\cdots\mathbf{r}_n)\rangle=\sum_{r_1\cdots r_N}^{N_0}F\prod_{i<j}^{N}g_{r_ir_j}\Big/\sum_{r_1\cdots r_N}^{N_0}\prod_{i<j}^{N}g_{r_ir_j}$$

$$=\sum_{r_1\cdots r_n}^{N_0}F\prod_{i<j}^{n}g_{r_ir_j}\Big/\sum_{r_1\cdots r_n}^{N_0}\prod_{i<j}^{n}g_{r_ir_j}.$$

We now expand the products of g's in the numerator of Eq. (A8) into sums of products of δ's keeping, however, the g's associated with u's in unexpanded form; i.e., we write $g_{r_ir_j}=(1-\delta_{r_ir_j})$ for all g's except those having the same indices as the u products. For example, we write

$$u_{r_1r_2}u_{r_3r_4}g_{r_1r_2}g_{r_3r_4}g_{r_1r_3}g_{r_1r_4}g_{r_2r_3}g_{r_2r_4}=u_{r_1r_2}u_{r_3r_4}g_{r_1r_2}g_{r_3r_4}(1-\delta_{r_1r_3})(1-\delta_{r_1r_4})(1-\delta_{r_2r_3})(1-\delta_{r_2r_4}). \quad \text{(A9)}$$

The diagrams in Fig. 7 denote how this is done. A solid line represents a factor $u_{r_ir_j}g_{r_ir_j}$ and a dashed line a factor $-\delta_{r_ir_j}$. The diagram of Fig. 7(d), for instance, represents the following expression (forgetting the denominator for the moment):

$$\sum u_{r_1r_2}u_{r_3r_4}g_{r_1r_2}g_{r_3r_4}\delta_{r_1r_3}\delta_{r_2r_3}\sum g_{r_1'r_2'}g_{r_3'r_4'}-\sum u_{r_1r_2}u_{r_3r_4}g_{r_1r_2}g_{r_3r_4}\sum g_{r_1'r_2'}g_{r_3'r_4'}\delta_{r_1'r_3'}\delta_{r_2'r_3'}$$
$$=\sum\delta_{r_1r_2}u_{r_1r_2}u_{r_3r_4}g_{r_1r_2}g_{r_3r_4}\sum g_{r_1'r_2'}g_{r_3'r_4'}-\sum u_{r_1r_2}u_{r_3r_4}g_{r_1r_2}g_{r_3r_4}\sum g_{r_1'r_2'}g_{r_2'r_4'}\delta_{r_1'r_2'}=0. \quad \text{(A10)}$$

In fact, the last three diagrams in Fig. 7 are identically zero because they contain at least one δ and u in parallel. When a diagram has two joined dashed lines coming from the ends of a single solid bond, it is identically zero. The first and second diagrams are also zero but for a different and more important reason. This is seen immediately when the numerator is written out.

$$\text{Figure 7(a)}=\sum u_{r_1r_2}u_{r_3r_4}g_{r_1r_2}g_{r_3r_4}\sum g_{r_1'r_2'}g_{r_3'r_4'}-\sum u_{r_1r_2}u_{r_3r_4}g_{r_1r_2}g_{r_3r_4}\sum g_{r_1'r_2'}g_{r_3'r_4'}=0, \quad \text{(A11)}$$

$$\text{Figure 7(b)}=\sum u_{r_1r_2}u_{r_3r_4}g_{r_1r_2}g_{r_3r_4}\delta_{r_1r_3}\sum g_{r_1'r_2'}g_{r_3'r_4'}-\sum u_{r_1r_2}u_{r_3r_4}g_{r_1r_2}g_{r_3r_4}\sum g_{r_1'r_2'}g_{r_3'r_4'}\delta_{r_1'r_3'}$$
$$=\sum u_{r_1r_2}u_{r_2r_3}g_{r_1r_2}g_{r_2r_3}\sum g_{r_1'r_2'}g_{r_3'r_4'}-\sum u_{r_1r_2}u_{r_3r_4}g_{r_1r_2}g_{r_3r_4}\sum g_{r_1'r_2'}g_{r_2'r_3'}$$
$$=(1/N_0)\sum u_{r_1r_2}u_{r_3r_4}g_{r_1r_2}g_{r_3r_4}\sum g_{r_1'r_2'}g_{r_3'r_4'}-(1/N_0)\sum u_{r_1r_2}u_{r_3r_4}g_{r_1r_2}g_{r_3r_4}\sum g_{r_1'r_2'}g_{r_3'r_4'}=0. \quad \text{(A12)}$$

The factorization occurring in Eq. (A12) is a result of the translational invariance of the u's. By this we mean that $\sum_{r_j=1}^{N_0} u_{r_i r_j} g_{r_i r_j}$ is independent of r_i. Hence, any term represented by a reducible graph will factorize in a manner similar to Eq. (A12) so that the full semi-invariant corresponding to such a reducible term will vanish. Finally, we are left with the third diagram which represents for the full expression in M_2

$$\text{Figure } 7(c)=1/D\Big[\sum_{i\neq j,\,k\neq l} u_{r_i r_j} u_{r_k r_l} g_{r_i r_j} g_{r_k r_l} \delta_{r_i r_k} \delta_{r_j r_l} \sum g_{r_i' r_j'} g_{r_k' r_l'} - u_{r_i r_j} u_{r_k r_l} g_{r_i r_j} g_{r_k r_l} \sum g_{r_i' r_j'} g_{r_k' r_l'} \delta_{r_i' r_k'} \delta_{r_j' r_l'}\Big], \quad \text{(A13)}$$

where

$$D=2\sum_{r_1\cdots r_4}^{N_0} \prod_{i<j=1}^{4} g_{r_i r_j} \sum_{r_1'\cdots r_4'}^{N_0} g_{r_1' r_2'} g_{r_3' r_4'}.$$

Equation (A13) is rewritten

$$\frac{1}{2}\frac{N(N-1)(N-2)(N-3)}{N_0(N_0-1)(N_0-2)(N_0-3)N_0^2(N_0-1)^2} \times\Big[N_0^2(N_0-1)^2 \sum_{r_1\cdots r_4} u_{r_1 r_2} u_{r_3 r_4}(-\delta_{r_1 r_3})(-\delta_{r_2 r_4}) g_{r_1 r_2} g_{r_3 r_4} - N_0(N_0-1)\sum_{r_1, r_2} u_{r_1 r_2} g_{r_1 r_2} \sum_{r_3, r_4} u_{r_3 r_4} g_{r_3 r_4}\Big] = \tfrac{1}{2} N_0 \rho^4 \sum g_{r_1 r_2}^2 u_{r_1 r_2}^2.$$

The second term in the numerator of Eq. (A13) is clearly $O(1/N_0)$ smaller than the first term.

The second term in Eq. (A7) yields the linked diagrams of Fig. 8. Figure 8(a) is zero through the argument following Eq. (A12) and Fig. 8(b) contributes to M_2;

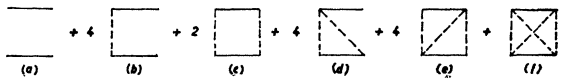

FIG. 7. Diagrams arising in M_2 from $u_{12}u_{34}$.

$$\text{Figure } 8(b)=\rho^3 \sum_{r_1 r_2 r_3} u_{r_1 r_2} g_{r_1 r_2} u_{r_2 r_3} g_{r_2 r_3} \times(-\delta_{r_1 r_3})=\rho^3 \sum_{r_1 r_2} u_{r_1 r_2}^2 g_{r_1 r_2}^2. \quad \text{(A14)}$$

Finally, the third term in Eq. (A7) contributes to M_2,

$$\text{Figure } 8(c)=\tfrac{1}{2}\rho^2 \sum_{r_1 r_2} u_{r_1 r_2}^2 g_{r_1 r_2}^2. \quad \text{(A15)}$$

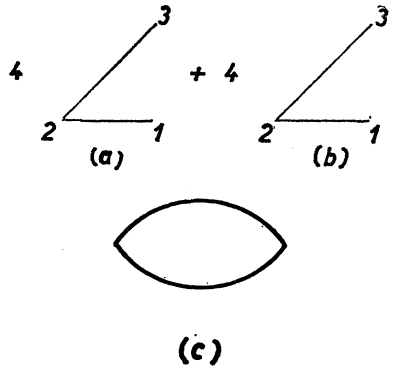

FIG. 8. Diagrams arising in M_2 from $u_{12}u_{23}$.

If we adopt the convention of calling a diagram irreducible if the irreducibility refers to dashed and solid lines together, then we have the result that for M_2, only irreducible diagrams contribute to the free energy. To prove the theorem that in general, only irreducible diagrams contribute to the free energy, we make use of Eq. (A1) for semi-invariants. Consider an unlinked diagram such as Fig. 9. Its contribution to M_6 is a cross term in the expression

$$M_6(u_{12}g_{12}+u_{24}g_{24}+u_{34}g_{34}+u_{13}g_{13}+u_{56}g_{56}-\delta_{14}). \quad \text{(A16)}$$

But $u_{56}g_{56}$ is independent of all the other terms in the argument of M_6 and, hence, by Eq. (A1) the cross term is zero. For clarity, we write out the cross term explicitly for $M_2(u_{12}g_{12}+u_{34}g_{34})$. This is

$$\sum_{r_1\cdots r_2} u_{r_1 r_2} g_{r_1 r_2} u_{r_3 r_4} g_{r_3 r_4} - \sum_{r_1 r_2} u_{r_1 r_2} g_{r_1 r_2} \sum_{r_3 r_4} u_{r_3 r_4} g_{r_3 r_4}. \quad \text{(A17)}$$

For reducibly linked terms, the above argument also holds, for consider the diagrams of Fig. 10. The contribution of Fig. 10(a) to M_6 is the cross term in

$$M_6(u_{12}g_{12}+u_{24}g_{24}+u_{34}g_{34}+u_{13}g_{13}-\delta_{14}+u_{25}g_{25}).$$

Again $u_{25}g_{25}$ is independent of the other terms in the argument of M_6 in the sense that

$$\sum u_{r_1 r_2} g_{r_1 r_2} u_{r_2 r_4} g_{r_2 r_4} u_{r_3 r_4} g_{r_3 r_4} u_{r_1 r_3} g_{r_1 r_3} \delta_{r_1 r_4} u_{r_2 r_5}^2 g_{r_2 r_5}^2 = (1/N_0) \sum_{r_1\cdots r_2} u_{r_1 r_2} g_{r_1 r_2} u_{r_2 r_4} g_{r_2 r_4} u_{r_3 r_4} g_{r_3 r_4} \times u_{r_1 r_3} g_{r_1 r_3} \delta_{r_1 r_4} \sum_{r_5 r_6} u_{r_6 r_6}^2 g_{r_5 r_6}^2. \quad \text{(A18)}$$

Hence, the contribution of Fig. 10(a) to the free energy is zero. The generalization is evident. Unlinked or re-

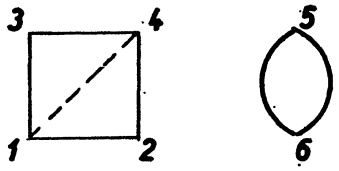

FIG. 9. A typical unlinked diagram occurring in M_6.

ducibly linked terms involve in their reduced parts, variables which are statistically independent. Hence, cross terms cannot appear involving such terms [Eq. (A1)]. Therefore, we have proved that all unlinked and reducibly linked diagrams are zero. Finally, it must be stated that only the first term of a semi-invariant expression for irreducible graphs is of $O(N)$ because all the other terms are partially unlinked and contain too many factors of δ_{ij} as in the second term of Eq. (A13).

It is not obvious that the cluster expansion which we have just derived is equivalent to the one originally obtained by Brout[1] for the Ising model since we have no semi-invariant expressions of $\epsilon_i\epsilon_j$. However, consider the four diagrams in third order (Fig. 11). When these diagrams are added together, we obtain

$$\begin{aligned}(-\rho^6+3\rho^5-3\rho^4+\rho^3)\sum u_{r_1r_2}u_{r_2r_3}u_{r_3r_1}&\\ =2^6(-\rho^6+3\rho^5-3\rho^4+\rho^3)\sum v_{r_1r_2}v_{r_2r_3}v_{r_3r_1}&\\ =(1-R^2)^3\sum v_{r_1r_2}v_{r_2r_3}v_{r_3r_1}.&\end{aligned}\tag{A19}$$

The factor "three" occurs because there are three ways of cutting a triangle and inserting one or two dashed lines in the vertices. Clearly, for a ring diagram of nth order, there are $\binom{n}{r}$ ways of inserting r dashed lines and since a dashed line carries a minus sign as well as a factor of ρ, we get for the sum of all ring graphs in nth order

$$\left[\rho^n-n\rho^{n-1}+\binom{n}{2}\rho^{n-2}+\cdots+(-1)^n\rho^{2n}\right]\sum u_{r_1r_2}\cdots u_{r_nr_1}$$
$$=[1-R^2]^n\sum v_{r_1r_2}\cdots v_{r_nr_1},\tag{A20}$$

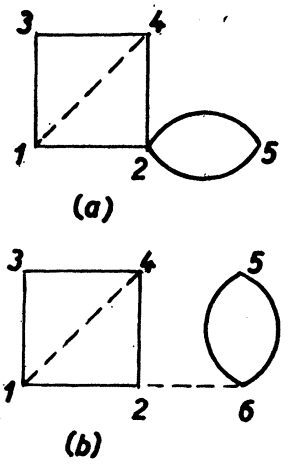

FIG. 10. Typical reducibly linked diagrams occurring in M_6.

which is the sum of the two ring diagrams (open and closed) in the nth order in Brout's expansion for the Ising model. It still appears that we have lost a great deal in this method since we have many more graphs in a given order than in Brout's expansion. However, we now prove the remarkable theorem that all external dashed line graphs in a given order belonging to the same configuration of u's can be summed and yield a surprisingly simple result similar to that obtained by Horwitz in IV. By way of introduction we first note that each vertex of a graph in any order can be broken up by inserting dashed lines. This is illustrated in Fig. 12. This holds regardless of what the solid lines are

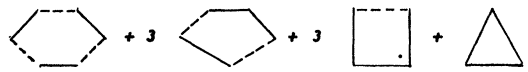

FIG. 11. The set of ring graphs in third order.

connected to. Thus, a skeleton graph which contains no dashed lines can be used to represent all graphs of the same type (i.e., configuration of u's) with dashed lines inserted in all the vertices. The value of the graph will be given by the product of polynomials with which each vertex is now associated times the appropriate expression in the u's. We now find the polynomial corresponding to a vertex of n lines. To do this, we first consider Fig. 12, a vertex with three lines. On the right-hand side of the arrow, the number of ways of obtaining the first and fourth graphs is one and the number of ways of obtaining the second and third graphs is three. Adding these together and remembering that a dashed line carries a minus sign, we get $\rho-3\rho^2+2\rho^3$. For a

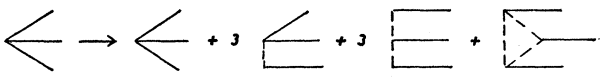

FIG. 12. Insertion of dashed lines in a three-line vertex.

four-line vertex, the expression is found to be $\rho-7\rho^2+12\rho^3+6\rho^4$. We now observe that the expression for a three-line vertex is just $M_3(\epsilon_i)=(\langle\epsilon_i^3\rangle-3\langle\epsilon_i^2\rangle\langle\epsilon_i\rangle+2\langle\epsilon_i\rangle^3)$ while the expression for a four-line vertex is

$$M_4(\epsilon_i)=(\langle\epsilon_i^4\rangle-4\langle\epsilon_i^3\rangle\langle\epsilon_i\rangle-3\langle\epsilon_i^2\rangle^2+12\langle\epsilon_i^2\rangle\langle\epsilon_i\rangle^2-6\langle\epsilon_i\rangle^4).$$

We, therefore, conjecture that the polynomial denoted by an n-line vertex is $M_n(\epsilon_i)$. We will prove this conjecture by induction. We first note that the coefficient of the term $\langle x^{n_1}\rangle^{\alpha_1}\langle x^{n_2}\rangle^{\alpha_2}\cdots\langle x^{n_s}\rangle^{\alpha_s}$ in $M_n(x)$ is

$$(-1)^{r-1}\frac{n!(r-1)!}{(n_1!)^{\alpha_1}(n_2!)^{\alpha_2}\cdots(n_s!)^{\alpha_s}\alpha_1!\alpha_2!\cdots\alpha_s!},\tag{A21}$$

where $\sum_{i=1}^s\alpha_in_i=n$; $\sum_{i=1}^s\alpha_i=r$. The number of ways of breaking up a vertex containing n lines into α_1, n_1's, α_2, n_2's, etc., is

$$\frac{n!}{(n_1!)^{\alpha_1}(n_2!)^{\alpha_2}\cdots(n_s!)^{\alpha_s}\alpha_1!\alpha_2!\cdots\alpha_s!}.\tag{A22}$$

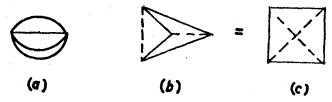

FIG. 13. Two equivalent diagrams in fourth order.

Also,

$$\langle \epsilon_i{}^n \rangle = \langle \epsilon_i \rangle = \rho, \tag{A23}$$

so that

$$\langle \epsilon_i{}^{n_1} \rangle^{\alpha_1} \langle \epsilon_i{}^{n_2} \rangle^{\alpha_2} \cdots \langle \epsilon_i{}^{n_s} \rangle^{\alpha_s} = \rho^r. \tag{A24}$$

Hence, it only remains to be shown that the number associated with the connection of r points by pairs such that each points is connected by at least one path to all the other points is $(-1)^{r-1}(r-1)!$. We assume that this result holds for r up to and equal to m. Now take $\rho=1$. This means that $\sum u_{ij}$ is constant since $N=N_0$. Then all terms in the expansion of the pressure vanish except the first semi-invariant. Consequently, the sum of the coefficients of each polynomial in ρ which we are considering vanishes and since the sum of the coefficients of any semi-invariant of higher order than one is zero, this implies that in a vertex containing $m+1$ lines, the coefficient of ρ^{m+1} is $(-1)^m m!$. Hence, by induction, the result is proved in general since it is obviously true for $r=2$. In the above proof, we have not considered internal dashed lines connected to the vertex under consideration. This introduces a complication in the proof but does not change the result. (See Appendix C.)

We can now state the general expansion for the pressure of the lattice gas. In the nth term, only irreducible solid line diagrams containing n solid lines remain. These irreducible solid line diagrams can contain only internal noncrossing dashed lines with the proviso that if we pinch a graph together where there is a dashed line, then the resulting graph must be a reducible one. The reason that only noncrossing internal dashed lines appear will be evident from the following example. Consider the irreducible diagram in fourth order as illustrated in Fig. 13(a). We can break the vertices up in the two manners indicated [Fig. 13(b) and Fig. 13(c)]. The equivalence of the two diagrams in Fig. 13 is obvious. Thus, in fourth order, the internal crossing dashed line diagram is already contained in the diagram, Fig. 13(a), with the convention that each vertex now represents a semi-invariant internal crossing dashed line diagram is contained in some other irreducible diagram and thus does not appear further. Furthermore, any other internal dashed line which when pinched leads to an irreducible diagram is not present in the expansion. An example will make this clear. Consider the diagram Fig. 14(a). This diagram is

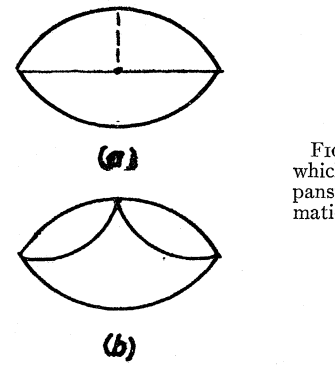

FIG. 14. Illustrative diagrams which appear in the cluster expansion due to vertex summation.

FIG. 15. Diagrams occurring in M_2.

already contained in the diagram, Fig. 14(b) and hence, should be omitted from the expansion. Another minor complication of vertex summation will be discussed in Appendix D. Disregarding this for the moment, we can state the final cluster expansion as follows. A diagram represents a structure of u's as before and, in addition, each vertex denotes a factor which is the νth semi-invariant of ϵ_i where ν is the number of solid lines joined to the vertex. All irreducible diagrams contribute except those with internal crossing dashed lines and those with internal dashed lines which when pinched yield irreducible diagrams. There are no external dashed line diagrams.

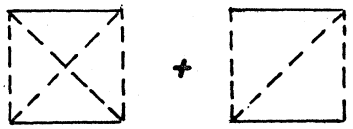

FIG. 16. Irreducible diagrams occurring in the cluster expansion of the real hard-core gas.

APPENDIX B

The starting point is Eq. (4.6). As before, we examine the first few semi-invariants:

$$\begin{aligned} M_1 &= \tfrac{1}{2}\langle \textstyle\sum v_{ij} \rangle = \tfrac{1}{2} \textstyle\sum \langle v_{ij} \rangle \\ &= \tfrac{1}{2} N(N-1) \langle v_{12} \rangle, \end{aligned} \tag{B1}$$

since $\langle v_{ij} \rangle$ is invariant for all $i \neq j$. Now

$$\begin{aligned} \langle v_{12} \rangle &= \frac{\int v(\mathbf{r}_1 - \mathbf{r}_2) \prod_{i<j=1}^{N} g(\mathbf{r}_i - \mathbf{r}_j) \prod d\mathbf{r}_i}{\int \prod_{i<j=1}^{N} g(\mathbf{r}_i - \mathbf{r}_j) \prod d\mathbf{r}_i} \\ &\equiv (1/V) \int v(\mathbf{r}) g^{(2)}(\mathbf{r}) d\mathbf{r}, \end{aligned} \tag{B2}$$

where we have introduced the two-particle hard-sphere distribution function $g^{(2)}(r)$ as defined in the canonical

ensemble

$$g^{(2)}(r)=\frac{V^2\int\prod_{i=3}^{N}d\mathbf{r}_i\prod_{i<j=1}^{N}g_{ij}}{\int\prod_{i=1}^{N}d\mathbf{r}_i\prod_{i<j=1}^{N}g_{ij}}. \tag{B3}$$

In the lattice gas, because of the simple nature of $W(\rho)$, all the integrals (sums) in the numerator and denominator except the first two of Eq. (B.2) cancel leaving

$$\langle v_{12}\rangle_{\text{L.G.}}=\frac{\sum_{r_1r_2=1}^{N_0}v_{\mathbf{r}_1\mathbf{r}_2}g_{\mathbf{r}_1\mathbf{r}_2}}{\sum g_{\mathbf{r}_1\mathbf{r}_2}}. \tag{B4}$$

This is just Eq. (A4). In the present case, there is no cancellation and it is evident that this will lead to difficulties in higher order semi-invariants. The second-order semi-invariant is

$$\begin{aligned}M_2&=\tfrac{1}{4}\sum_{i<j=1}^{N}[\langle v_{ij}v_{kl}\rangle-\langle v_{ij}\rangle\langle v_{kl}\rangle]\\&=\tfrac{1}{4}\sum_{i\neq j\neq k\neq l}^{N}[\langle v_{ij}v_{kl}\rangle-\langle v_{ij}\rangle\langle v_{kl}\rangle]\\&\quad+\sum_{i\neq j\neq k}^{N}[\langle v_{ij}v_{jk}\rangle-\langle v_{ij}\rangle\langle v_{jk}\rangle]\\&\quad+\tfrac{1}{2}\sum_{i\neq j}^{N}[\langle v_{ij}^2\rangle-\langle v_{ij}\rangle^2].\end{aligned} \tag{B5}$$

Let us examine the first term in square brackets in the right-hand side of Eq. (B5),

$$\begin{aligned}&\langle v_{12}v_{34}\rangle-\langle v_{12}\rangle\langle v_{34}\rangle\\&=\frac{\int v_{12}v_{34}\prod g_{ij}\prod d\mathbf{r}_i}{\int\prod g_{ij}\prod d\mathbf{r}_i}\\&\quad-\frac{\int v_{12}\prod g_{ij}\prod d\mathbf{r}_i\int v_{34}\prod g_{kl}\prod d\mathbf{r}_k}{\int\prod g_{ij}\prod d\mathbf{r}_i\int\prod g_{kl}\prod d\mathbf{r}_k}.\end{aligned} \tag{B6}$$

The canonical distribution function for n particles is defined by

$$g^{(n)}=\frac{V^n\int\prod_{i=n+1}^{N}d\mathbf{r}_i\prod g_{ij}}{\int\prod_{i=1}^{N}d\mathbf{r}_i\prod g_{ij}}. \tag{B7}$$

Putting this into Eq. (4.12), we get

$$\begin{aligned}&\langle v_{12}v_{34}\rangle-\langle v_{12}\rangle\langle v_{34}\rangle\\&=(1/V^4)\Big\{\int\prod_{i=1}^{4}d\mathbf{r}_iv_{12}v_{34}[g^{(4)}(\mathbf{r},\mathbf{r}_2,\mathbf{r}_3,\mathbf{r}_4)\\&\qquad-g^{(2)}(\mathbf{r}_1,\mathbf{r}_2)g^{(2)}(\mathbf{r}_3,\mathbf{r}_4)]\Big\}.\end{aligned} \tag{B8}$$

By a result first proved by Mayer and Montroll[16] and rederived in a simpler fashion by Meeron,[17] the n-particle distribution function can be written as an expansion in the density,

$$g^{(n)}=\sum_{\nu=0}^{\infty}\rho^\nu/\nu!\,g_\nu^{(n)}(\mathbf{r}_1\cdots\mathbf{r}_n), \tag{B9}$$

where

$$g_\nu^{(n)}(\mathbf{r}_1\cdots\mathbf{r}_n)=\prod_{i<j=1}^{n}g_{ij}(\mathbf{r}_i-\mathbf{r}_j)\int P(n,\nu)\prod_{i=n+1}^{n+\nu}d\mathbf{r}_i, \tag{B10}$$

$P(n,\nu)$ denotes the sum of all products of functions $f_{ij}(\mathbf{r}_i-\mathbf{r}_j)=1-g_{ij}(\mathbf{r}_i-\mathbf{r}_j)$ in which each particle of the set ν is independently connected to at least two particles of the set n, ν and n being mutually exclusive. The bonds in this connection are the functions $-f_{ij}(\mathbf{r}_i-\mathbf{r}_j)$. A particle is independently connected to two others if there are at least two paths, either direct or involving mutually exclusive sets of intermediate particle, which connect it to the two others.

To make further progress, we shall at this point introduce the superposition approximation of Kirkwood.[8] According to Eqs. (B9) and (B10), Fig. 17 is an

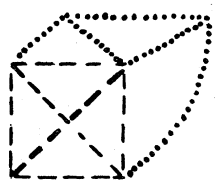

FIG. 17. Diagram contributing to $g^{(4)}(r_1,r_2,r_3,r_4)$.

example of a diagram contribution to $g^{(4)}$. The dashed lines denote $g_{ij}(\mathbf{r}_i-\mathbf{r}_j)$ bonds and the dotted lines denote $-f_{ij}(\mathbf{r}_j-\mathbf{r}_j)$ bonds.[18] Calling the points 1, 2, 3, 4 base points and all other points field points, we now make the approximation of taking only those diagrams in which field points which are connected either directly or indirectly to two given base points are connected to each other but not to field points which are connected to different base points. Alternatively two field points connected to two given base points are not connected to each other by an intermediate base point. This is in fact the superposition approximation for n base

[16] J. Mayer and E. Montroll, J. Chem. Phys. **9**, 300 (1941).
[17] E. Meeron, J. Chem. Phys. **27**, 1238 (1957).
[18] The reader should note that this use of the dashed line is unique to the discussion of superposition as illustrated in Fig. 17. All other dashed lines in this section will mean $\tilde{f}(r_i-r_j)$.

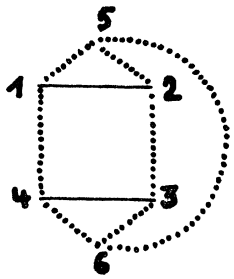

FIG. 18. A nonsuperposition diagram.

points. In superposition approximation, $g^{(n)}(\mathbf{r}_1\cdots\mathbf{r}_n)$ is given by $\prod_{i<j} g_{ij}^{(2)}$.

To get an idea of the order of magnitude of what we are throwing away, consider the graph Fig. 18. If we define the cube of the range of the potential $v(r)$ to be the volume v_s, then v_s/v_a is comparable to the parameter z, the number of nearest neighbors in the lattice gas. Taking v_s/v_a to be large, we see that the diagram of Fig. 18 is $O(v_a/v_s)^2$. This is so because each solid bond (i.e., a factor ρv) is $O(v_a/v_s)$ [i.e., $(1/z)$] as we shall see from the molecular field theory. The integration over $\mathbf{r}_1$, $\mathbf{r}_2$, $\mathbf{r}_3$, $\mathbf{r}_4$ gives a factor of $O(v_s/v_a)$. Furthermore, since points 5 and 6 are connected, this limits the range of points 3 and 2 to the neighborhood of points 1 and 4. This further reduces the order of

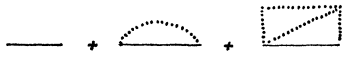

FIG. 19. Diagram contributing to $v(r)g^{(2)}(r)$.

magnitude of the diagram by a factor so that we obtain $O[(v_a/v_s)^2]$ for the diagram. This is evidently the simplest type of diagram which we are not including in the expansion.

To see that more complicated nonsuperposition graphs are $O[(v_a/v_s)^2]$ we first notice that according to Eqs. (B9) and (B10) a solid line which carries the totality of dotted lines drawn between its ends simply becomes $v_{ij}(\mathbf{r}_i-\mathbf{r}_j)g^{(2)}(\mathbf{r}_i-\mathbf{r}_j)$ (Fig. 19). We then note that the set of graphs in Fig. 20 yields the function $-[1-g^{(2)}(\mathbf{r}_i-\mathbf{r}_j)]$ which we denote by $-\tilde{f}(\mathbf{r}_i-\mathbf{r}_j)$. From now on, solid lines will be used to represent $v_{ij}(\mathbf{r}_i-\mathbf{r}_j)g^{(2)}(\mathbf{r}_i-\mathbf{r}_j)$ and dashed lines to represent $-\tilde{f}(\mathbf{r}_i-\mathbf{r}_j)$. If we now replace the dotted line connecting points 5 and 6 in Fig. 18 by a dashed line, then the reasoning following Fig. 18 still holds since $\tilde{f}(\mathbf{r})$ is just $f(\mathbf{r})$ with a highly damped oscillating tail. We have thus shown that a particular class of nonsuperposition graphs is of $O[(v_a/v_s)^2]$. As it is easy to construct other geometries in lowest order where this is the case, we may then surmise that there are no nonsuperposition

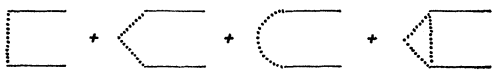

FIG. 20. Diagram contributing to a graph containing $\tilde{f}(r)$.

graphs of order greater than $(v_a/v_s)^2$. We have not attempted a general proof at this point.

We now outline the method whereby irreducible graphs are obtained for the free energy in superposition approximation. The first few graphs from Eq. (B8) which arise in the density expansion of $g^{(4)}(r_1,r_2,r_3,r_4)$ are presented in Fig. 21 where we temporarily use a solid line to denote $v(\mathbf{r})g(\mathbf{r})$. Consider now Fig. 22 which is contained in the sum represented by Fig. 21. It would appear at first that this diagram would contribute to $v_{12}(\mathbf{r}_1-\mathbf{r}_2)v_{34}(\mathbf{r}_3-\mathbf{r}_4)\tilde{f}(\mathbf{r}_1-\mathbf{r}_3)\tilde{f}(\mathbf{r}_1-\mathbf{r}_4)$ but since $v_{12}(\mathbf{r}_1-\mathbf{r}_2)$ can be integrated out (i.e., the diagram is reducible), it actually contributes to $v_{12}(\mathbf{r}_1-\mathbf{r}_2)\times v_{34}(\mathbf{r}_3-\mathbf{r}_4)g^{(2)}(\mathbf{r}_3-\mathbf{r}_4)$. It is then obvious that there

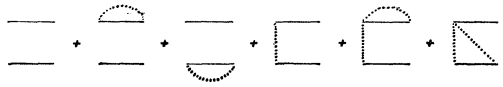

FIG. 21. Density expansion of Eq. (B8).

are no diagrams which will contribute to $v_{12}(\mathbf{r}_1-\mathbf{r}_2)\times v_{34}(\mathbf{r}_3-\mathbf{r}_4)f(\mathbf{r}_1-\mathbf{r}_3)f(\mathbf{r}_1-\mathbf{r}_4)$ or any other reducible combination involving two f's. This is a general result. Whenever there are two or more pieces connected by a reducible combination of dashed lines, such a graph is to be discarded. See Appendix E for the proof of this statement. The first term in Eq. (B8) is now seen to be

$$v_{12}v_{34}g_{12}^{(2)}g_{34}^{(2)}[g_{13}^{(2)}g_{14}^{(2)}g_{23}^{(2)}g_{24}^{(2)} - \tilde{f}_{13}\tilde{f}_{14} - \tilde{f}_{13}\tilde{f}_{23} - \tilde{f}_{23}\tilde{f}_{24} - \tilde{f}_{14}\tilde{f}_{24}] \equiv v_{12}v_{34}\prod_{i<j=1}^{4}{}' g_{ij}^{(2)}, \quad \text{(B11)}$$

where the prime over the product indicates that we must subtract all the reducible combinations involving

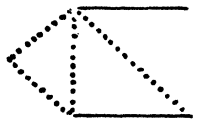

FIG. 22. Reducible diagram contained in the density expansion of Eq. (B8).

two f's from the product of $g^{(2)}$'s indicated. Equation (B8) can now be written

$$\langle v_{12}v_{34}\rangle - \langle v_{12}\rangle\langle v_{34}\rangle = \frac{1}{V^4}\left\{\int \prod_{i=1}^{4} d\mathbf{r}_i\, v_{12}v_{34}\Big[\prod_{i<j=1}^{4}{}' g_{ij}^{(2)} - g_{12}^{(2)}g_{34}^{(2)}\Big]\right\}. \quad \text{(B12)}$$

As in the case of the lattice gas, we expand the product (primed) of $g^{(2)}$'s into sums of products of f's keeping the $g^{(2)}$'s associated with v's. Thus, the possible graphs which may arise in M_2 are given by Fig. 15. Notice that in Eq. (B12), there are no denominators as there were in Eq. (A8) for the lattice gas. This is a

consequence of the definition of $g^{(n)}(r_1\cdots r_n)$ by Eq. (B7). According to this definition,

$$\int g^{(2)}(\mathbf{r}_1-\mathbf{r}_2)d\mathbf{r}_1d\mathbf{r}_2=V^2, \tag{B13}$$

$$\int g^{(2)}(\mathbf{r})d\mathbf{r}=V, \tag{B14}$$

or

$$\int d\mathbf{r}\,\tilde{f}(\mathbf{r})=\int(1-g^{(2)}(\mathbf{r}))d\mathbf{r}=0. \tag{B15}$$

It is an immediate consequence of Eq. (B15) together with the factorizability properties of unlinked and reducibly linked portions of a graph that all unlinked and reducibly linked diagrams are zero. The proof is the same as that for the lattice gas.

We thus find that using the generalized superposition approximation, the expansion for the pressure contains all irreducible graphs of solid and dashed line bonds where a solid line denotes a $v_{ij}(\mathbf{r}_i-\mathbf{r}_j)g^{(2)}(\mathbf{r}_i-\mathbf{r}_j)$ bond and a dashed line denotes the $\tilde{f}(\mathbf{r}_i-\mathbf{r}_j)$ bond. A graph represents an integral over the bonds which it contains multiplied by ρ^m times a combinatorial factor which is the number of ways of obtaining the graph in the semi-invariant expansion. Here, m denotes the number of vertices and n the number of solid lines in the graph. The expansion is thus the same as the lattice gas cluster expansion before vertex summation with the addition of irreducible diagrams of the type in Fig. 16 and with the pair correlation function, $g^{(2)}(\mathbf{r}_i-\mathbf{r}_j)$ used in place of $g_{\mathbf{r}_i\mathbf{r}_j}$ and $\tilde{f}(\mathbf{r}_i-\mathbf{r}_j)$ used in place of $\delta_{\mathbf{r}_i\mathbf{r}_j}$.

APPENDIX C

One complication arises in the proof that each vertex of a graph denotes a semi-invariant. This complication exists when there is an internal dashed line connected to a vertex as in the graph of Fig. 23 which shows one of the vertices containing a dashed line being opened up. If the dashed line were not present, there would be only one external dashed line diagram. However, we see that the three external dashed line diagrams in Fig. 7 add up to the same value $(1+1-1=1)$ as an external dashed line diagram with a single dashed line connected to it. This is shown in Fig. 24. Furthermore, when there are n internal dashed lines connected to a vertex, each intenral dotted line gives rise to three graphs (if the vertex contain two solid lines) when the vertex is opened up. There are thus 3^n graphs formed when a vertex containing two dashed lines is opened up.

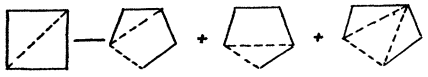

FIG. 23 Insertion of a dashed line in a vertex containing an internal dashed line.

FIG. 24. Value of the diagrams of Fig. 7.

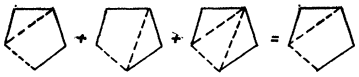

But the value of the renormalized vertex is simply the product of the values of the graphs formed by each of the n dotted lines which is $(-1)^n$. This is just the value of an unrenormalized vertex containing n internal dashed lines. Hence, for a vertex containing two solid lines with any number of internal dashed lines connected to it the value obtained when we renormalize is just the semi-invariant, $M_2(\epsilon_i)$. In the case of a vertex containing more than two solid lines, we again consider one internal dashed line connected to it. When the vertex is broken up, we must replace the single internal dashed line by $1\cdots r$, dashed lines if the vertex containing n solid lines is broken into r pieces. The number of ways of arranging m lines or r vertices is $\binom{r}{m}$. Summing this on m gives the value of an n-line vertex broken up into r pieces. This is just

$$\sum_{m=1}^{r}(-1)^m\binom{r}{m}=-1, \tag{C1}$$

which again is just the value of the vertex with only one dashed line connected to it. If we consider l internal dashed lines connected to an n-line vertex, we simply get $(-1)^1$ regardless of how many pieces the vertex is broken into. This shows that the procedure of renormalizing each vertex of a diagram by summing all external dashed line diagrams having that vertex is unaffected by internal dashed lines connected to the vertex.

APPENDIX D

A minor complication occurs in connection with the vertex summation of lattice graphs. Consider the diagrams of Fig. 25. They each have the same configura-

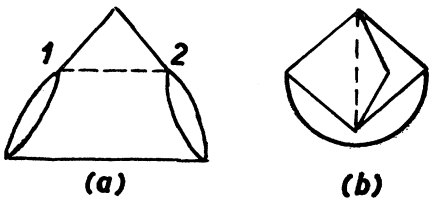

FIG. 25. Unrenormalized diagrams contributing to M_7.

tion of u's and also the same symmetry factor of $\frac{1}{8}$. This is arrived at for the diagram of Fig. 25(a) by

$$\binom{1}{7!}\binom{7}{5}\binom{4!}{2}\times5\times2\times\tfrac{1}{2}\times\tfrac{1}{2}=\tfrac{1}{8}, \tag{D1}$$

and for the diagram of Fig. 17(b) by

$$\binom{1}{7!}\binom{7}{5}\binom{5}{4}\times\binom{3!}{2}\times 2=\tfrac{1}{8}. \qquad \text{(D2)}$$

Now it is possible by inserting dashed lines at vertices 1 and 2 of each diagram to arrive at the same diagram. This is done in the manner indicated in Fig. 26. Consider Fig. 26(a) occurring in the cluster expansion. This diagram has a symmetry factor of $\frac{1}{2}$ which is obtained by

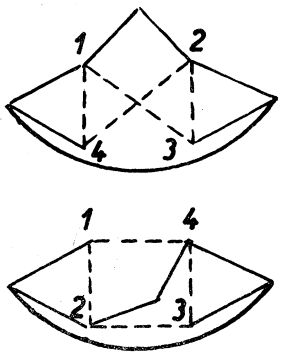

FIG. 26. Identical diagrams produced by breaking up diagrams 17(a) and 17(b).

$$\frac{1}{7!}\binom{7}{5}\frac{4!}{2}\times 5\times 2=\tfrac{1}{2}. \qquad \text{(D3)}$$

But Fig. 26(a) can be obtained in four ways and Fig. 26(b) in two ways so that it appears that we have overcounted this diagram by our method of breaking up vertices. That this is not the case will now be shown. Consider the points 1, 2, 3, and 4 in Figs. 26(a) and 26(b). In Fig. 26(a), points 1 and 4 must be connected together as well as points 2 and 3. In Fig. 26(b), the same thing holds. Consequently, in order to have identical diagrams, we must have at least the vertices indicated in Fig. 27 joined together in Fig. 26(a). Therefore, identical diagrams occur only for those diagrams obtained from Fig. 26(a) in which the vertices are joined as in Fig. 28. But the sum of the four diagrams in which the vertices are joined as in Fig. 28 is zero. Therefore, in breaking up Figs. 25(a) and 25(b) at least, there is no overcounting. We therefore conjecture (but cannot prove) that the vertex summation as stated in Appendix A does not lead to overcounting. In any case, any given class of graphs can be examined as we have done above.

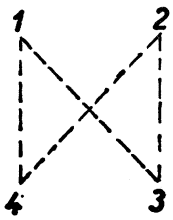

FIG. 27. Vertices in Fig. 18(a) which must be joined to have identical diagrams from Figs. 17(a) and 17(b).

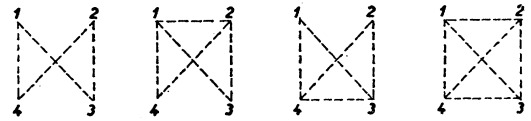

FIG. 28. Ways of joining vertices to produce identical diagrams.

APPENDIX E

In connection with Eq. (B11) it was stated that the diagram of Fig. 22 contributed to $v_{12}v_{34}g_{34}^{(2)}$. The proof of this statement and a general proof for reducible diagrams in all orders follows. We consider first the following diagrams in second and third order. If the diagrams of Fig. 29(a) are considered together, then the contribution is to $v_{12}v_{34}g_{34}^{(2)}$ and the full semi-invariant expression is zero. To see this we write down what the diagrams of Fig. 29(a) stand for being careful with the factors of N involved. The two diagrams of Fig. 29(a) are

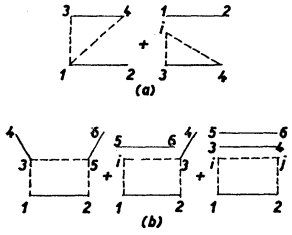

FIG. 29. Diagrams contributing to second and third orders.

$$\frac{N(N-1)(N-2)(N-3)}{V^4}\Big\{2\int d^3r_1\cdots d^3r_4\, v_{12}v_{34}f_{13}f_{14}$$
$$+\frac{1}{V}\sum_{i=5}^{N}\int d^3r_i d^3r_1\cdots d^3r_4\, v_{12}v_{34}f_{3i}f_{i4}-\frac{1}{V}\sum_{i=3}^{N}\int d^3r_i d^3r_1\cdots d^3r_4\, v_{12}v_{34}f_{3i}f_{i4}\Big\}$$
$$=\frac{N(N-1)(N-2)(N-3)}{V^5}\int v_{12}v_{34}f_{35}f_{45}d^3r_1\cdots d^3r_5[2+(N-4)-(N-2)]=0. \qquad \text{(E1)}$$

Similarly, for the diagrams of Fig. 29(b), we have

$$\frac{N(N-1)(N-2)(N-3)(N-4)(N-5)}{V^6}\Big\{8\int v_{12}v_{34}v_{56}f_{13}f_{35}f_{25}\prod_{i=1}^{6}d^3\mathbf{r}_i$$

$$+\frac{8}{V}\sum_{i=7}^{N}\int v_{12}v_{34}v_{56}f_{1i}f_{i3}f_{32}\prod_{j=1}^{6}d^3\mathbf{r}_j d^3\mathbf{r}_i+\frac{1}{V}\sum_{i\neq j=7}^{N}\int v_{12}v_{34}v_{56}f_{1i}f_{ij}f_{j2}\prod_{k=1}^{6}d^3\mathbf{r}_k d^3\mathbf{r}_i d^3\mathbf{r}_j$$

$$-2\times\frac{4}{V}\sum_{i=5}^{N}\int v_{12}v_{34}v_{56}f_{1i}f_{i3}f_{32}\prod_{j=1}^{6}d^3\mathbf{r}_j d^3\mathbf{r}_i+\frac{1}{V}\sum_{i\neq j}^{N}\int v_{12}v_{34}v_{56}f_{1i}f_{ij}f_{j2}\prod_{k=1}^{6}d^3\mathbf{r}_k d^3\mathbf{r}_i d^3\mathbf{r}_j$$

$$-\frac{1}{V}\sum_{i\neq j=3}^{N}\int v_{12}v_{34}v_{56}f_{1i}f_{ij}f_{j2}\prod_{k=1}^{6}d^3\mathbf{r}_k d^3\mathbf{r}_i d^3\mathbf{r}_j+\frac{2}{V}\sum_{i\neq j=3}^{N}\int v_{12}v_{34}v_{56}f_{1i}f_{ij}f_{j2}\prod_{k=1}^{6}d^3\mathbf{r}_k d^3\mathbf{r}_i d^3\mathbf{r}_j\Big\}$$

$$=\frac{N(N-1)(N-2)(N-3)(N-4)(N-5)}{V^8}\int\prod_{i=1}^{8}d^3\mathbf{r}_i v_{12}v_{34}v_{56}f_{17}f_{78}f_{82}$$

$$\times\{8+8(N-6)+(N-6)(N-7)-2[4(N-4)+(N-4)(N-5)]-(N-2)(N-3)+2(N-2)(N-3)\}=0. \quad \text{(E2)}$$

In fact, it is obvious that we are dealing with semi-invariants of independent variables. For instance, Eq. (E1) can be written as

$$\frac{N(N-1)(N-2)(N-3)}{V^4}\sum_{i=3}^{N}[\langle v_{12}f_{1i}f_{i2}v_{34}\rangle-\langle v_{12}f_{1i}f_{i2}\rangle\langle v_{34}\rangle]=0, \quad \text{(C3)}$$

while Eq. (C2) can be written as

$$\frac{N(N-1)(N-2)(N-3)}{V^4}\sum_{\substack{i\neq j=3\\ i=j\ j=4\ i=5\ j=6\\ i=4\ j=3\ i=6\ j=5\}\text{excluded}}^{N}[\langle v_{12}v_{34}v_{56}f_{1i}f_{ij}f_{j2}\rangle-\langle v_{12}f_{1i}f_{ij}f_{j2}v_{34}\rangle\langle v_{56}\rangle$$

$$-\langle v_{12}f_{1i}f_{ij}f_{j2}v_{56}\rangle\langle v_{34}\rangle-\langle v_{12}f_{1i}f_{ij}f_{j2}\rangle\langle v_{34}v_{56}\rangle+2\langle v_{12}f_{1i}f_{ij}f_{j2}\rangle\langle v_{34}\rangle\langle v_{56}\rangle]=0.$$

Consequently, every diagram involving reducible combinations of f and v bonds is zero when the full semi-invariant is taken into account. We must consider these diagrams then to contribute to some $g^{(2)}$ bond rather than to a product of $\tilde{f}$ bonds as in the above examples.